Title: Post-Merger Gravitational Wave Emission

Date: Jun 11, 2018 11:30 AM

URL: http://pirsa.org/18060046

Abstract:

Heidelberg Institute for Theoretical Studies

HITS

Postmerger gravitational wave emission

Path to Kilohertz Gravitational-Wave Astronomy, Perimeter Institute, Waterloo, 11/06/2018

Andreas Bauswein

(Heidelberg Institute for Theoretical Studies)

with K. Chatziioannou, J. A. Clark, H.-T. Janka, O. Just, N.Stergioulas

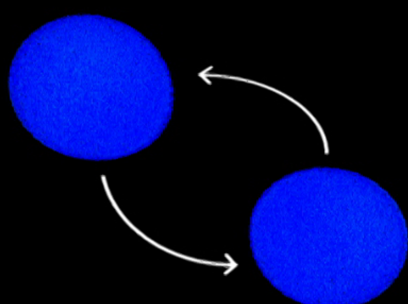

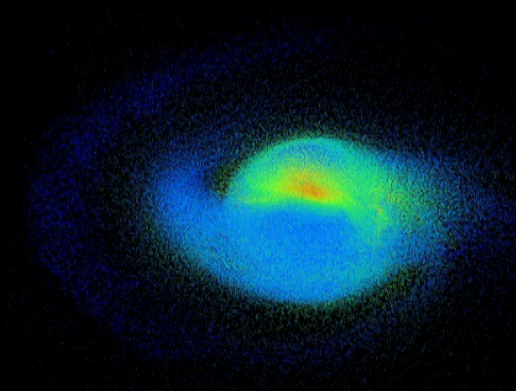

Time scales

- Neutron stars are among the most exciting objects in the Universe – not only for astophysics, but many more fields beyond
- Dynamical time scale of 1.4 Msun neutron stars (rotation period similar):

$$t_{\mathrm{dyn}} = \sqrt{\frac{R^3}{G\,M}} \approx 2\ ms$$

=> ***kHz*** Gravitational-Wave Astronomy

Outline

- Motivation / Introduction
- Dominant postmerger frequency

  → NS radius measurements

  → GW data analysis
- Secondary features of the postmerger GW spectrum

  → unified picture of postmerger dynamics and GW emission

  → EoS dependence
- Collapse behavior

  → NS radius constraints

  [→ Maximum mass]
- Conclusions and summary

Motivation: kHz GW emission

- Learn about unknown properties of high-density matter
- Link postmerger dynamics and multi-messenger picture: em counterpart, r-process, ...

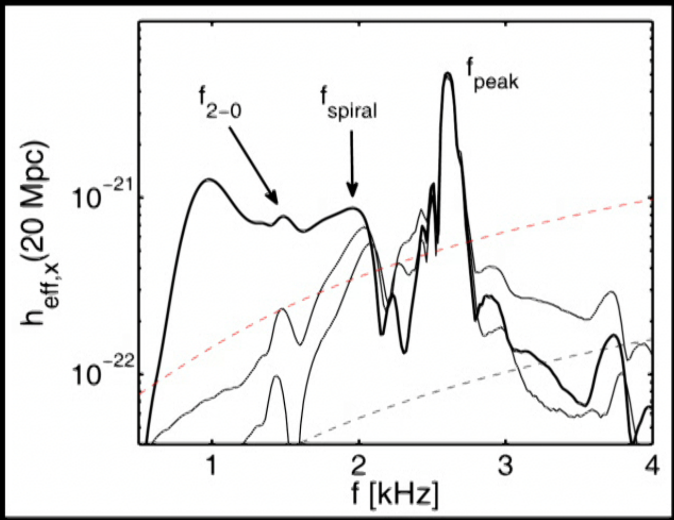

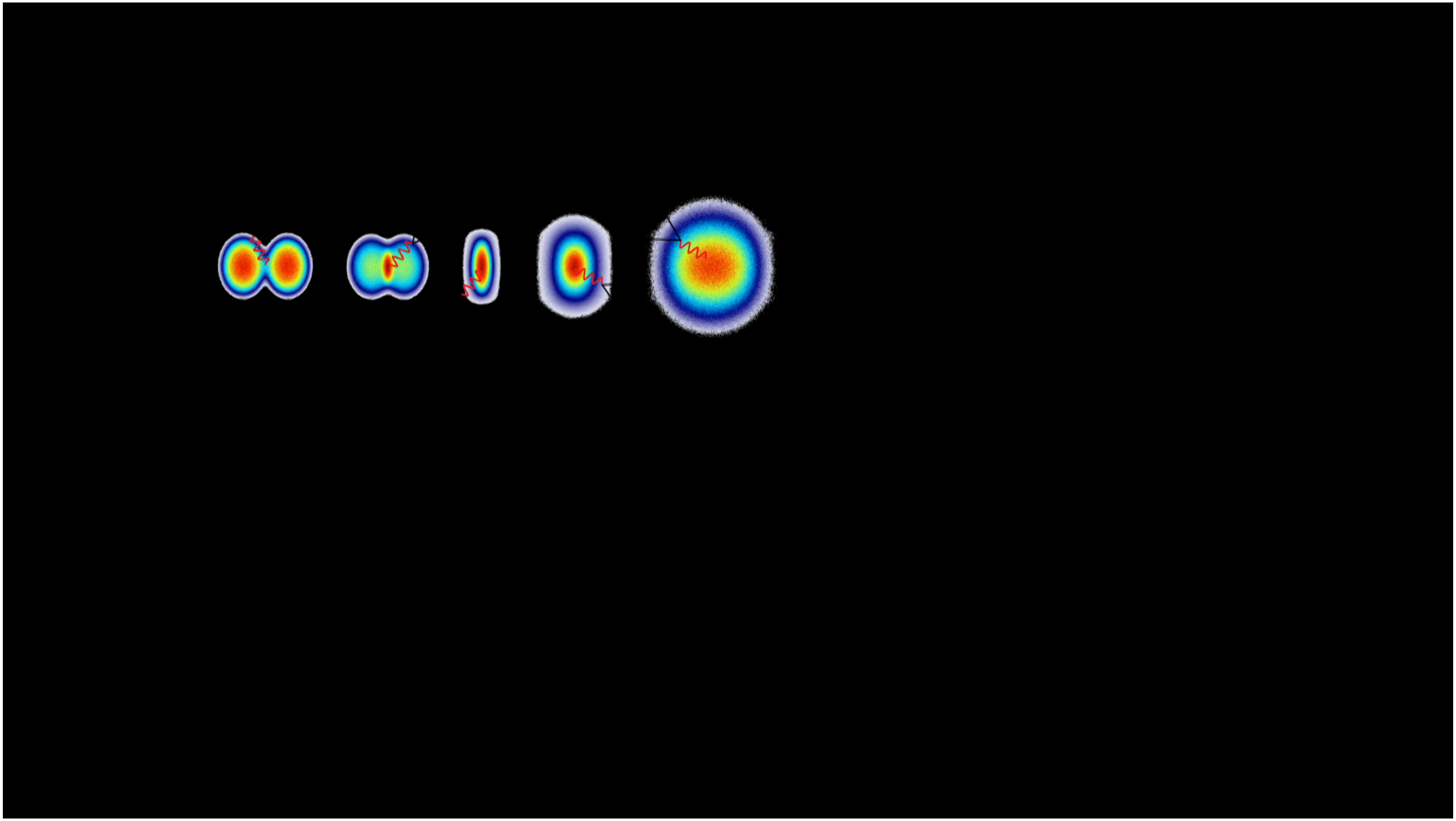

Phasediagram of matter

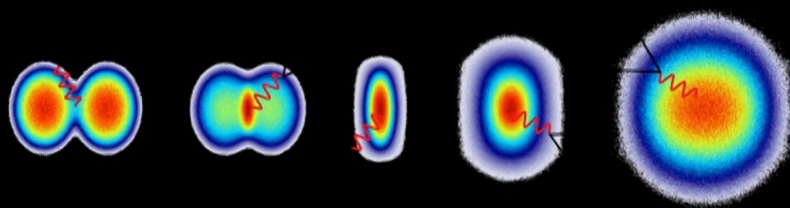

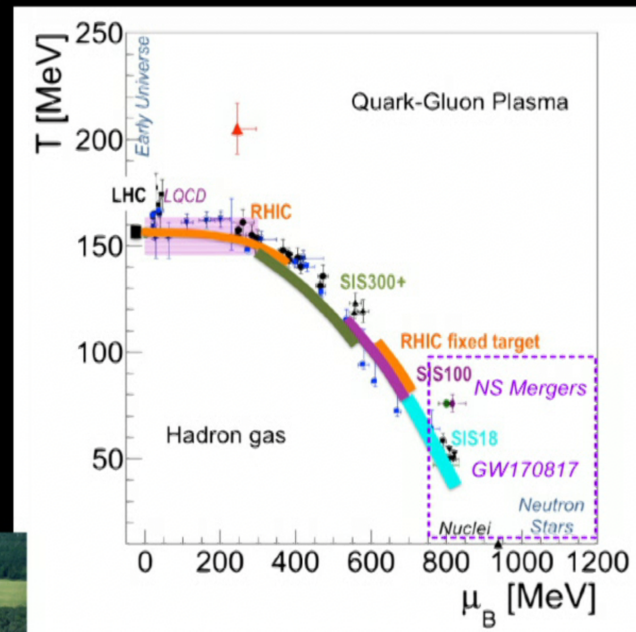

Many experiments world-wide trying to access high-density (high temperature) regime of matter through heavy-ion collisions, e.g. CBM @ FAIR

The EoS of high-density matter

- NSs and the high-density EoS

  - properties of nuclear matter (stiffness) – determine nuclear parameters

  - fundamental constituents hyperons, kaons, ...

  - deconfinement quark matter → understand confinement

  - EoS also critical for many astrophysical phenomena: supernovae, NS cooling, ...

  → determine NS radii – uniquely linked to EoS

- Postmerger (= kHz) GWs are similar and complimentary to inspiral methods

  → properties of cold EoS (e.g. NS radii, tidal deformability) → important to cross-check inspiral results (still plagued by systematics)

  → probe higher density regime

  → access to hot temperature

Introductory remark

- Mass-radius relation (of non-rotating NSs) and EoS are uniquely linked through Tolman-Oppenheimer-Volkoff (TOV) equations

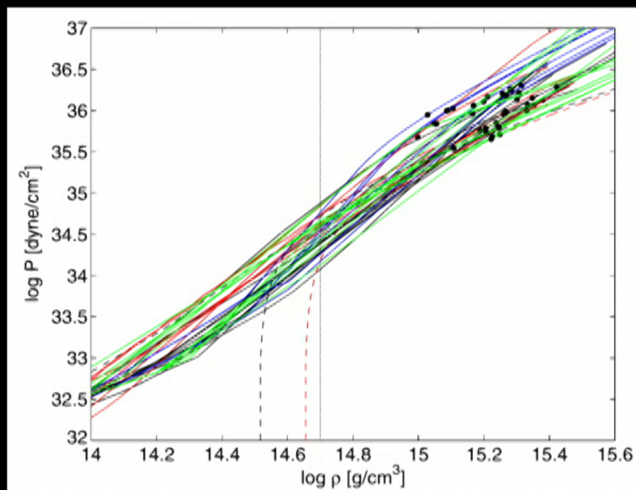

TOV ⟷

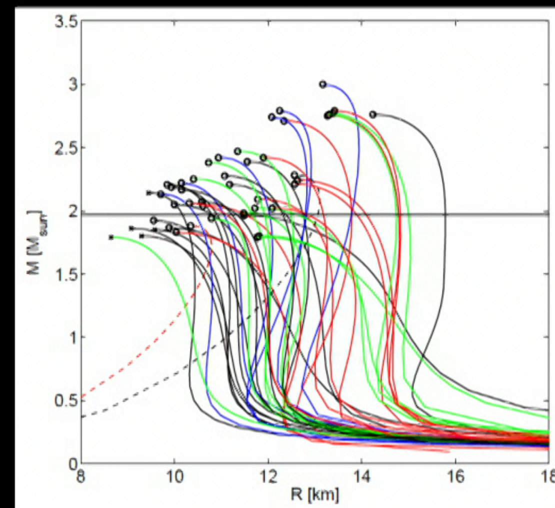

Theory: P(ρ) ⟷ (currently / future) Observation: R(M)

→ NS properties (of non-rotating stars) and EoS properties are equivalent !!!

(not all displayed EoS compatible with all current constraints)

Mass ejection - Simulations

$L_{\mathrm{bol}} \propto \sqrt{M_{\mathrm{ejecta}}}$

Dots trace ejecta (DD2 EoS 1.35-1.35 M_{sun})

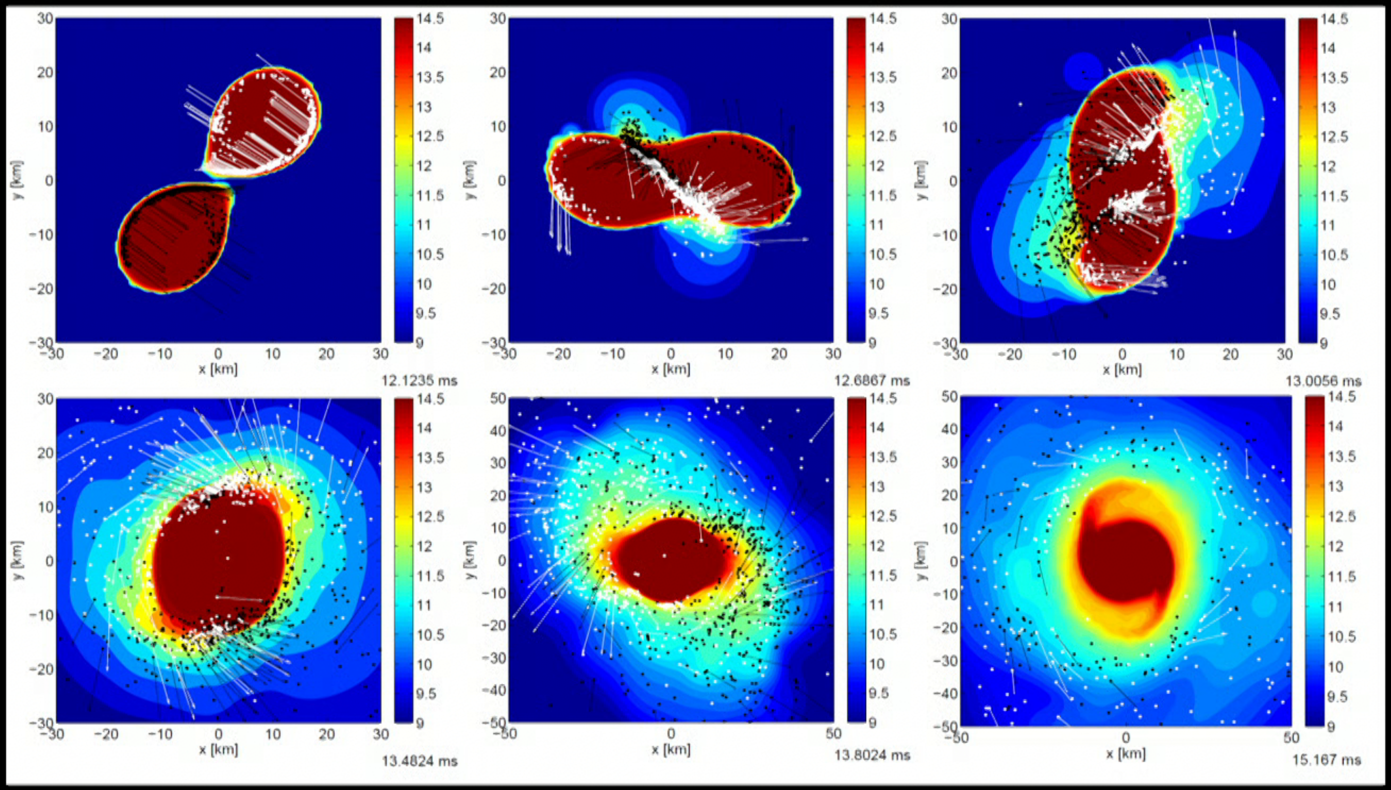

Bauswein et al. 2013

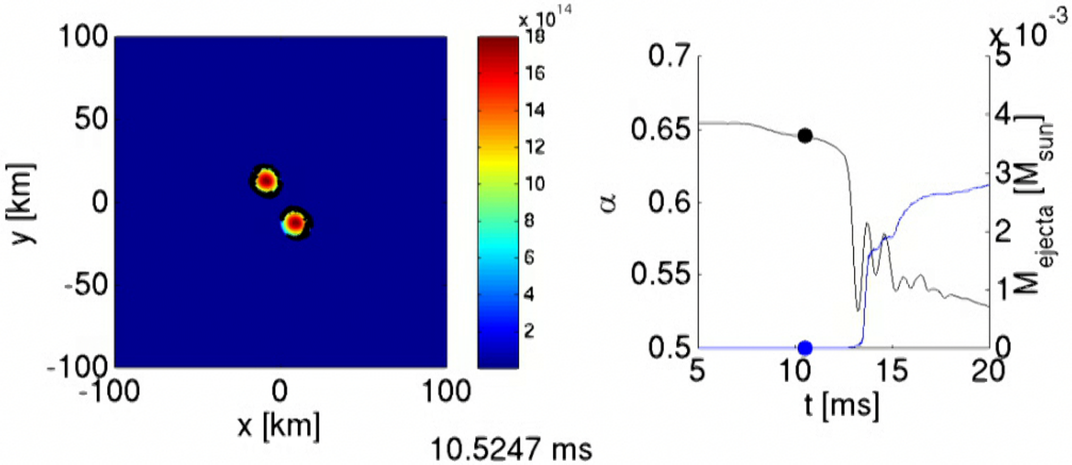

Black: bound; white: unbound (formally)

Central lapse: measure for compactness

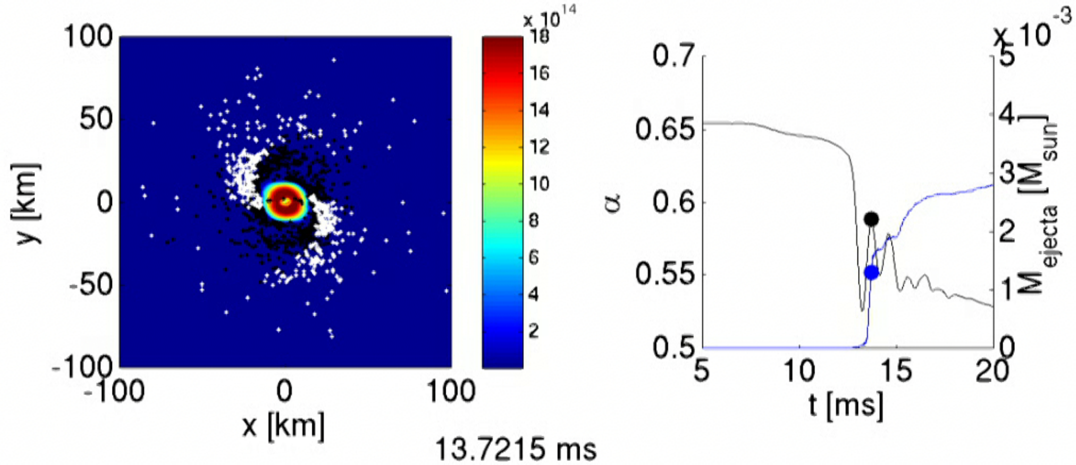

Black: bound; white: unbound (formally)

Central lapse: measure for compactness

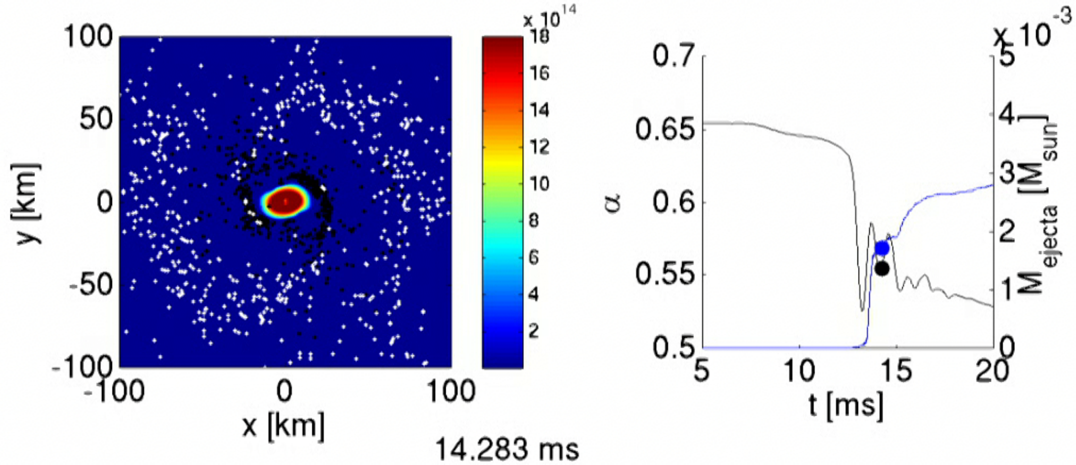

Black: bound; white: unbound (formally)

Central lapse: measure for compactness

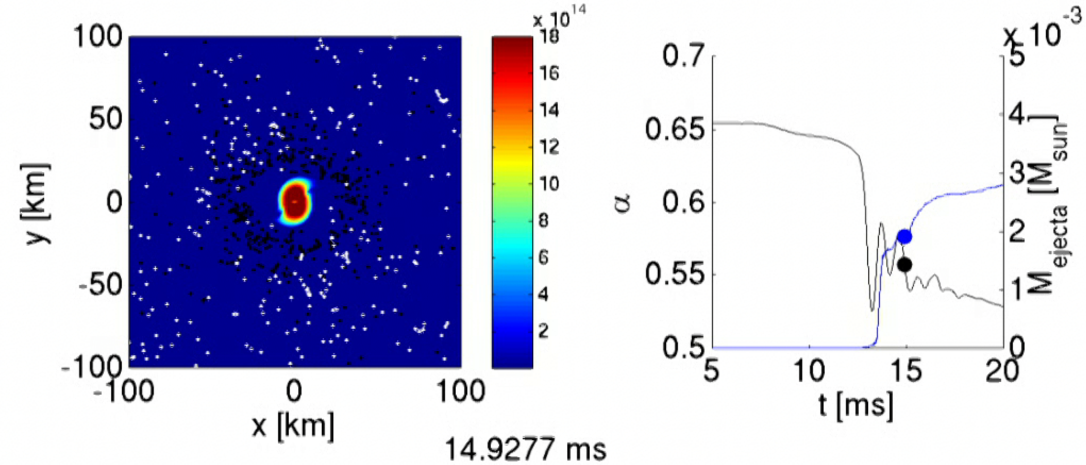

Black: bound; white: unbound (formally)

Central lapse: measure for compactness

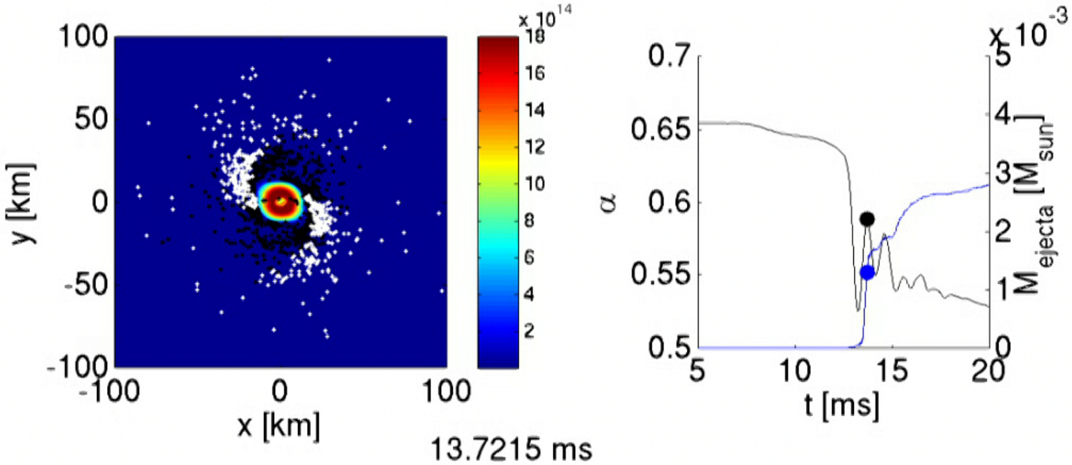

Black: bound; white: unbound (formally)

Central lapse: measure for compactness

Ejecta mass dependencies: binary para.

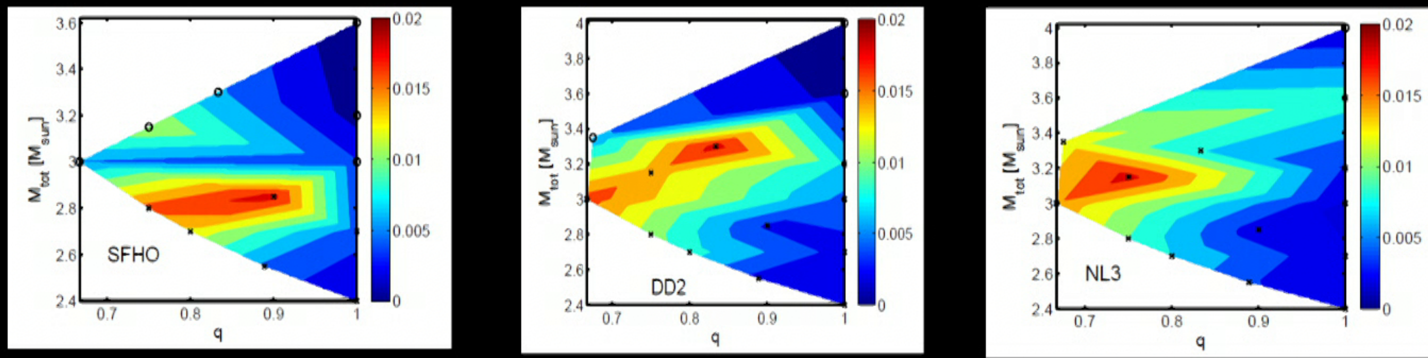

Stiffness

understandable by different dynamics / impact velocity / postmerger oscillations

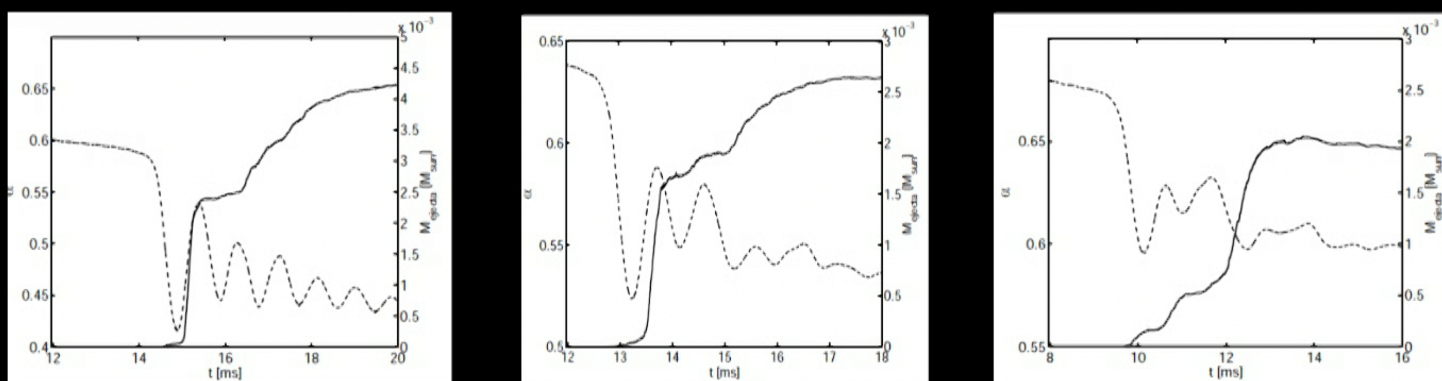

Central lapse α traces remnant compactness / oscillations / dynamics (dashed lines)

Ejecta mass dependence

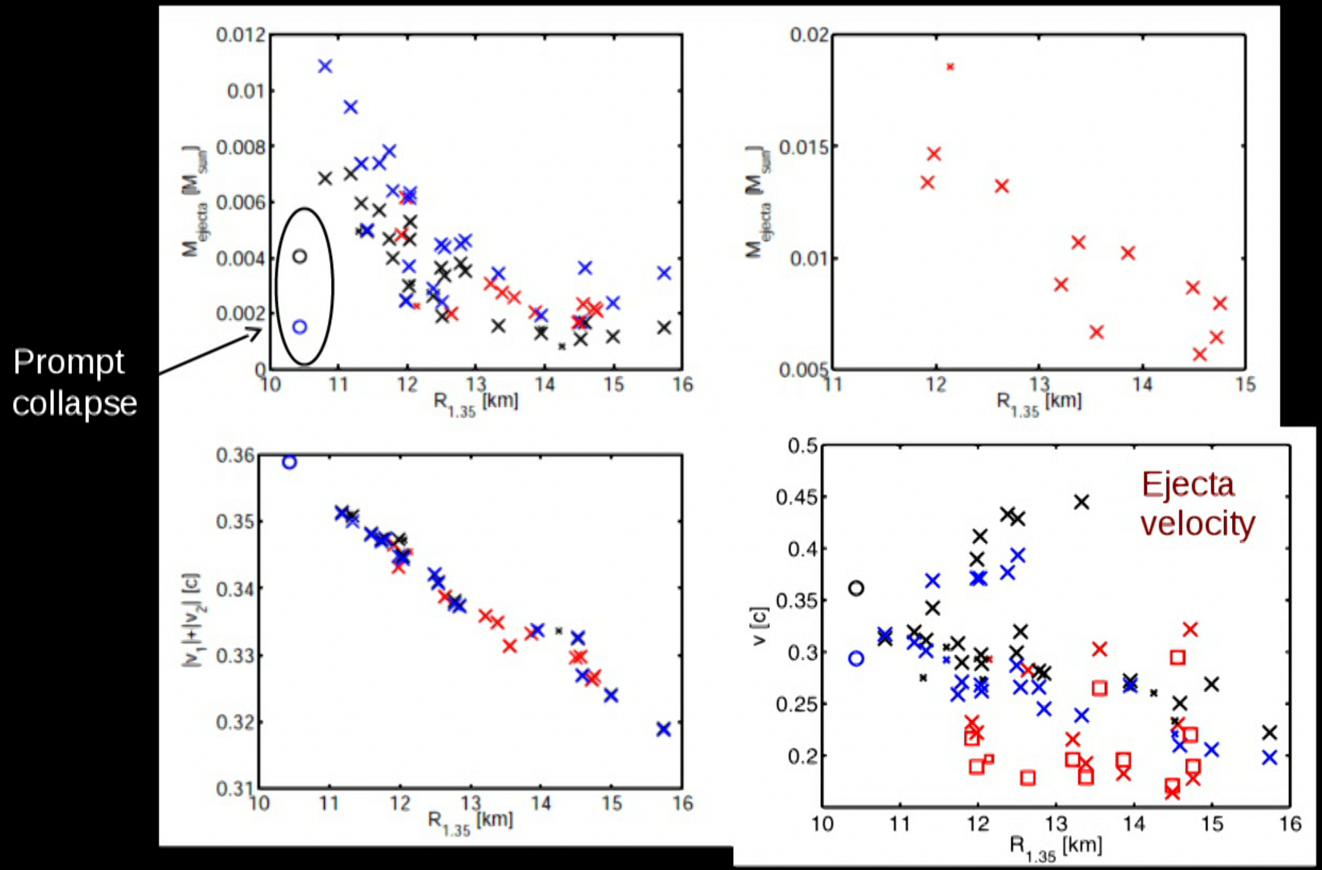

Different EoSs characterized by radii of 1.35 M_{sun} NSs (note importannce of thermal effects)

Outlook: postmerger dynamics and outcome accessible by kHz GWs

- Mass ejection → em counterpart (incl GRB) depends critically on collapse behavior

  → postmerger – kHz – GW emission will tell nature of remnant

- kHz GWs encode dynamics of postmerger remnant

  → should be reflected in properties of em counterpart → details to be worked out

  → multi-messenger astronomy

Dominant postmerger emission:

Radius measurements

Typical GW spectrum

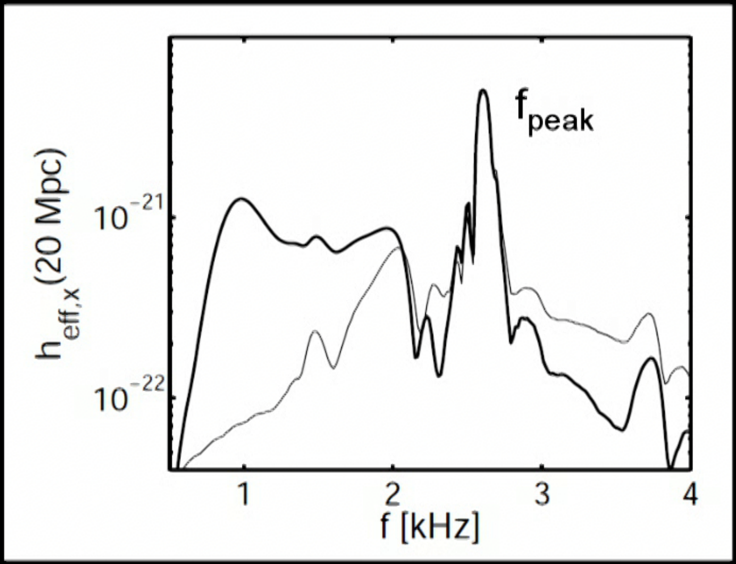

Thin line postmerger only

Note: no unique nomenclature in the literature, e.g. f_{peak} is also called f_2 …

- Up to 3 pronounced features in postmerger spectrum (f_{peak} + up to two secondary peaks at lower frequencies (subdominant wrt to sensitivity curve; not always present) + structure at higher frequencies)
- f_{peak} robust feature present in all models leading to a NS remnant
- Focus on f_{peak} – in comparison the easiest to measured
- Simulation: 1.35-1.35 M_{sun} DD2 EoS, Smooth Particle Hydro, Conformal Flatness

Gravitational waves – EoS survey

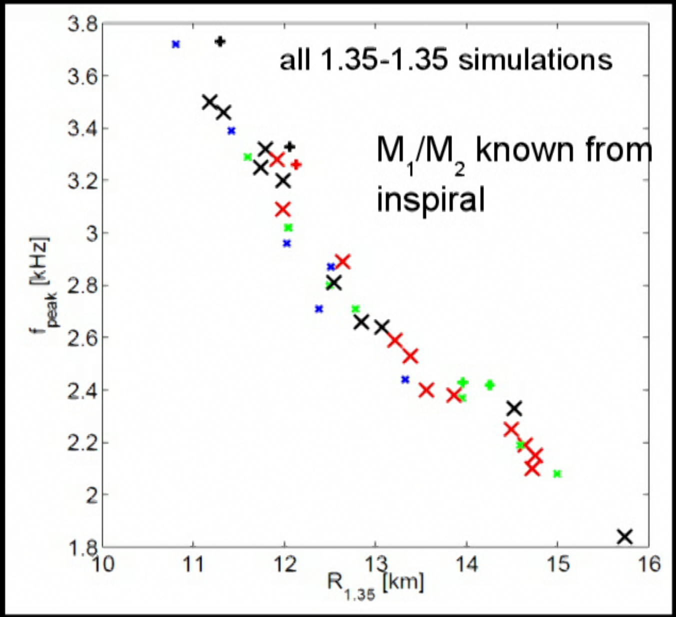

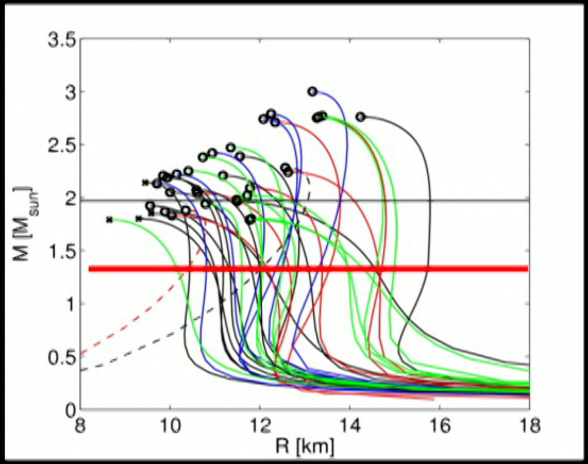

characterize EoS by radius of nonrotating NS with 1.35 M_{sun}

Bauswein et al. 2012

Pure TOV/EoS property => Radius measurement via f_{peak}

Here only 1.35-1.35 Msun mergers (binary masses measurable) – similar relations exist for other fixed binary setups !!!

~ 40 different NS EoSs

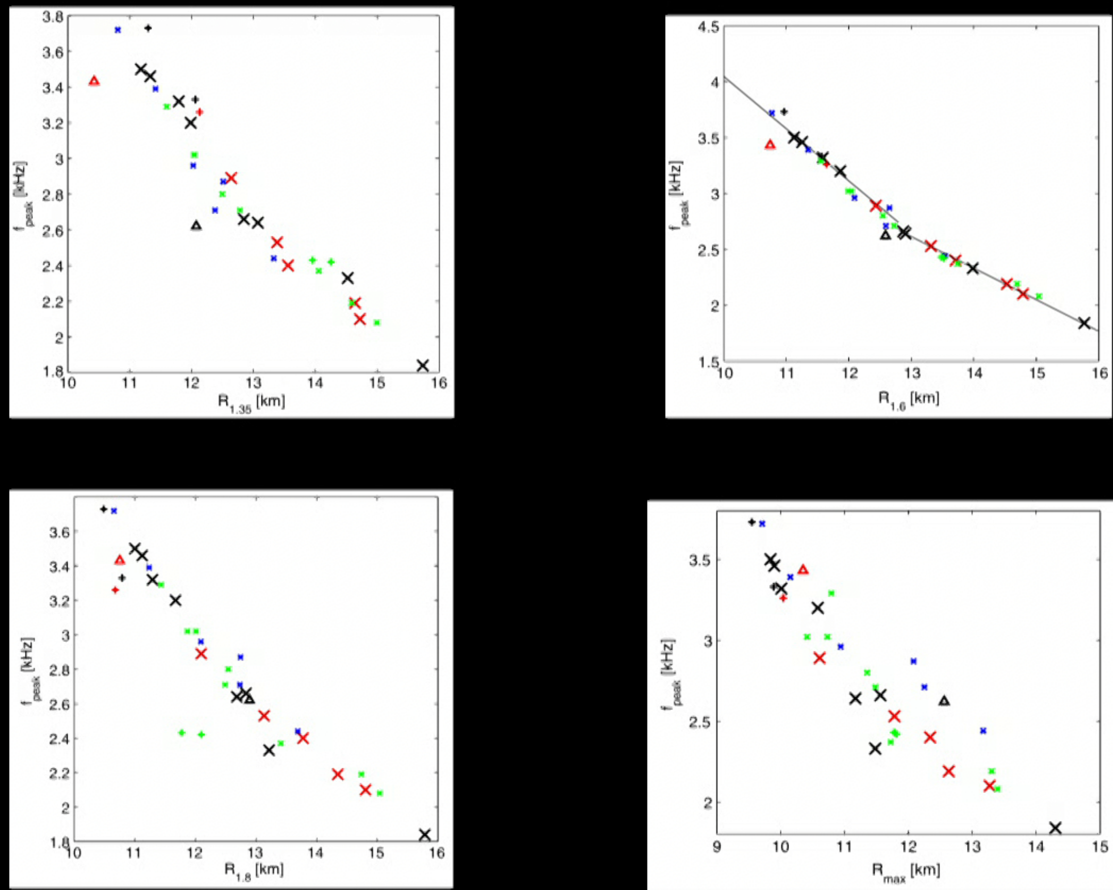

Bauswein et al. 2012

Assess quality of empirical relation relation – only infinity norm meaningful !!!

→ as many EoS models as possible !!!

Gravitational waves – EoS survey

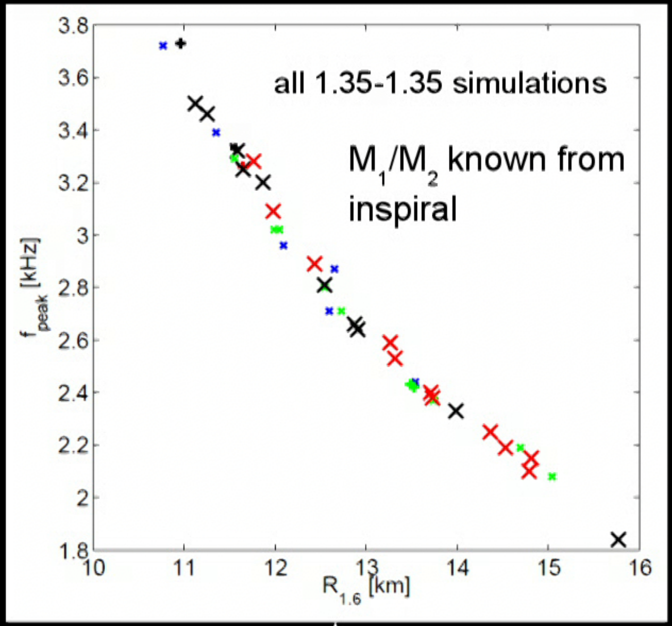

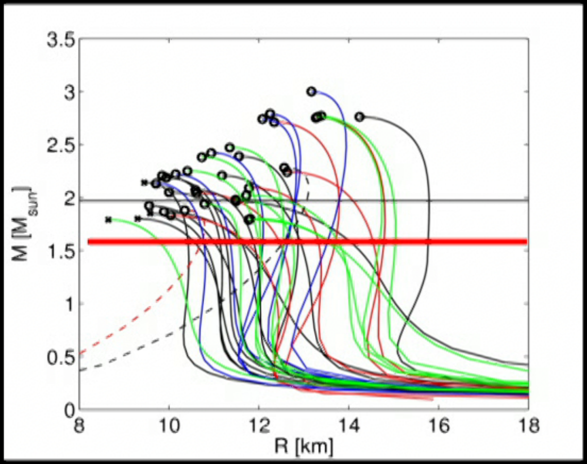

characterize EoS by radius of nonrotating NS with 1.6 M_{sun}

Bauswein et al. 2012

Pure TOV/EoS property => Radius measurement via f_{peak}

Smaller scatter in empirical relation (< 200 m) → smaller error in radius measurement

Note: R of 1.6 M_{sun} NS scales with f_{peak} from 1.35-1.35 M_{sun} mergers (density regimes comparable)

Binary mass variations

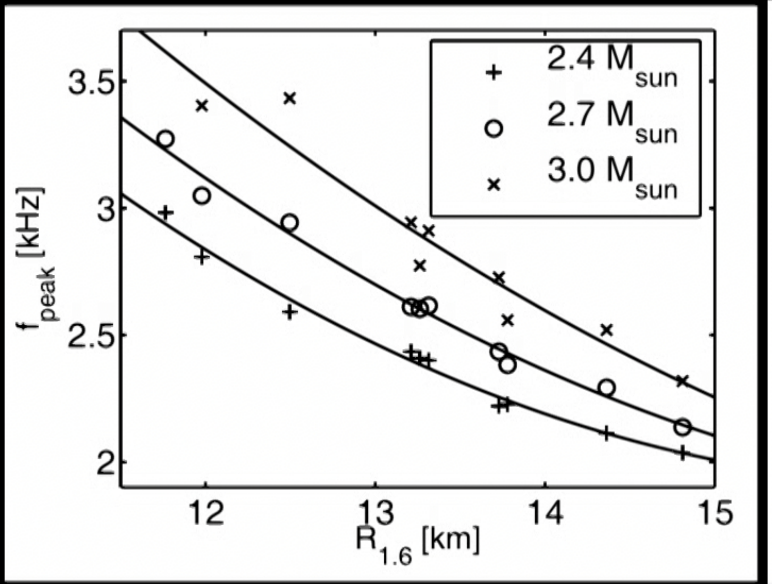

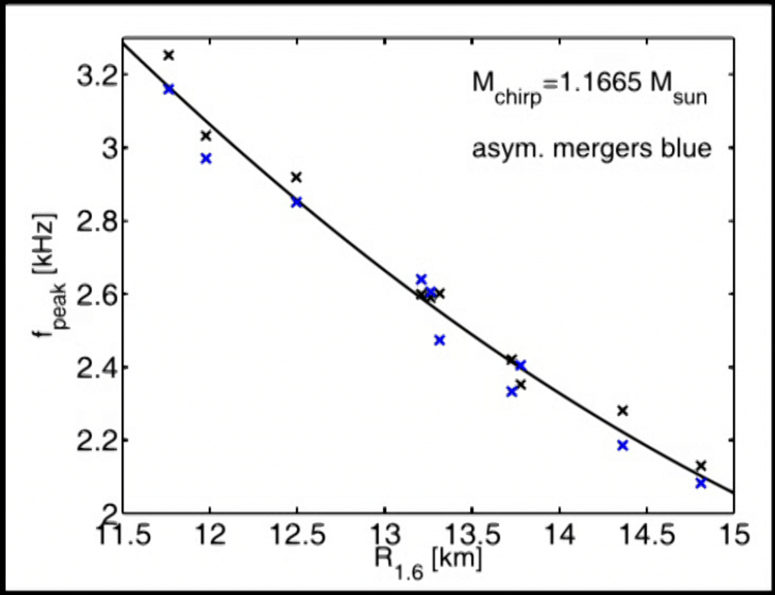

Different total binary masses (symmetric)

Fixed chirp mass (asymmertic 1.2-1.5 M_{sun} binaries and symmetric 1.34-1.34 M_{sun} binaries)

Data analysis: see Clark et al. 2016 (PCA), Clark et al. 2014 (burst search), Chatziioannou et al 2017, Yang et al 2018, Bose et al. 2018

→ f_{peak} precisely measurable !!!

Bauswein et al. 2012, 2016

Strategy for radius measurements

- Measure binary masses from inspiral
- Construct f_{peak} – R relation for this fixed binary masses and (optimally) chosen R
- Measure f_{peak} from postmerger GW signal
- Obtain radius by inverting f_{peak} – R relation
- (possibly restrict to fixed mass ratios if mergers with high asymmetry are measured)

- Final error of radius measurement:

  - accuracy of f_{peak} measurement (see Clark et al. 2014, Clark et al. 2016, ...)

  - maximum scatter in f-R relation (important to consider very large sample of EoSs)

  - systematic error in f-R relation

Data analysis

- Principal Component analysis

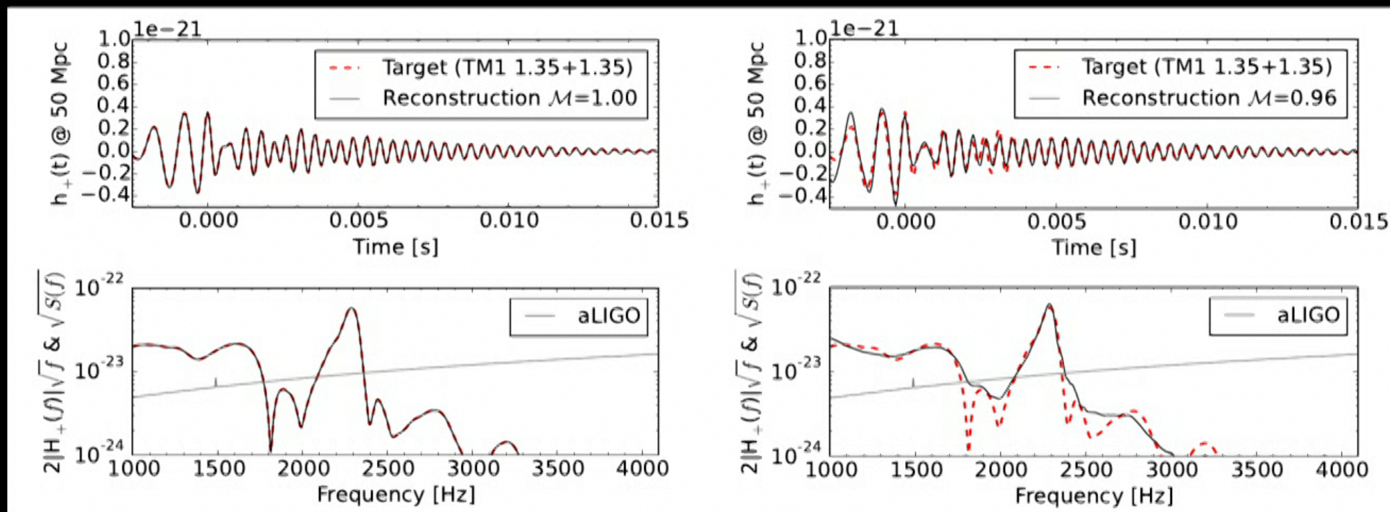

Excluding recovered waveform from catalogue

Instrument	SNR_{full}	D_{hor} [Mpc]	$\dot{N}_{det}$ [year^{-1}]
aLIGO	$2.99^{3.86}_{2.37}$	$29.89^{38.57}_{23.76}$	$0.01^{0.03}_{0.01}$
A+	$7.89^{10.16}_{6.25}$	$78.89^{101.67}_{62.52}$	$0.13^{0.20}_{0.10}$
LV	$14.06^{18.13}_{11.16}$	$140.56^{181.29}_{111.60}$	$0.41^{0.88}_{0.21}$
ET-D	$26.65^{34.28}_{20.81}$	$266.52^{342.80}_{208.06}$	$2.81^{5.98}_{1.33}$
CE	$41.50^{53.52}_{32.99}$	$414.62^{535.221}_{329.88}$	$10.59^{22.78}_{5.33}$

Outdated!!!

→ possible at Ad. LIGO's design sensitivity !!!

Clark et al. 2016, see also
Clark et al 2014,
Chatziioannou et al 2017,
Bose et al. 2018,
Yang et al. 2018

Secondary GW features and postmerger dynamics *

→ potentially EoS constraints
→ details of postmerger dynamics

* - for one-arm spiral instability see e.g. East et al 2016, Lehner et al 2016, …
- also CFS unstable modes may grow, e.g. Doneva et al 2015

Dominant oscillation frequency

- Robust feature, which occurs in all models (which don't collapse promptly to BH)
- Fundamental quadrupolar fluid mode of the remnant

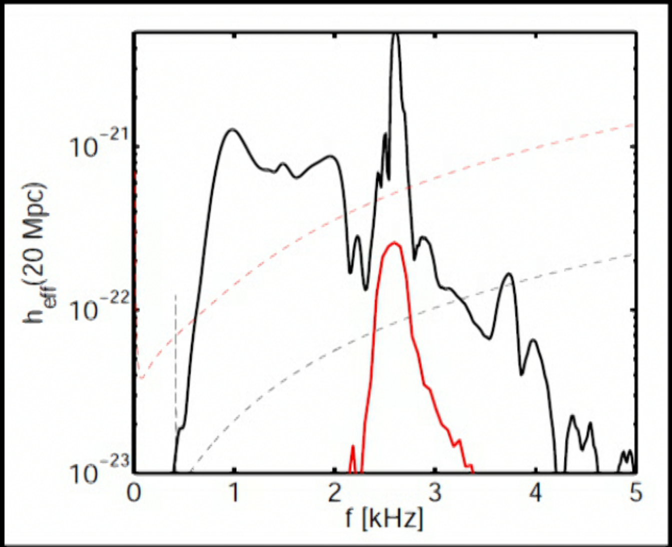

Re-excitation of f-mode (l=|m|=2) in late-time remnant (Bauswein et al. 2016)

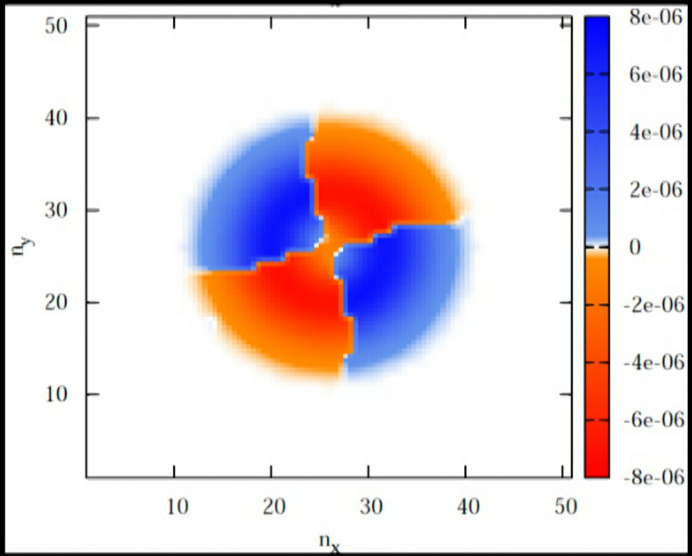

Mode analysis at $f=f_{peak}$ Stergioulas et al. 2011

Generic GW spectrum

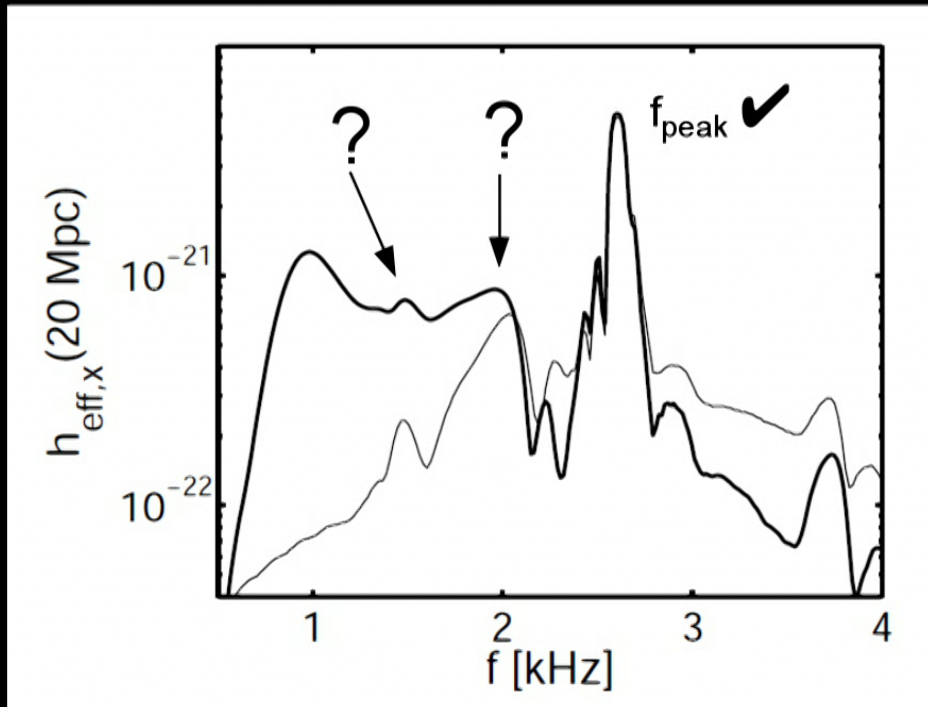

- Up to three pronounced features in the postmerger spectrum (+ structure at higher frequencies)
- 1.35-1.35 Msun DD2 EoS

Quasi-radial mode

- Central lapse function shows two frequencies (~500 Hz and ~1100 Hz) → clear peaks in FFT
- Add quasi-radial perturbation → re-excite quasi-radial mode => f_0 = 1100 Hz
- Confirmed by mode analysis → radial eigen function at f_0

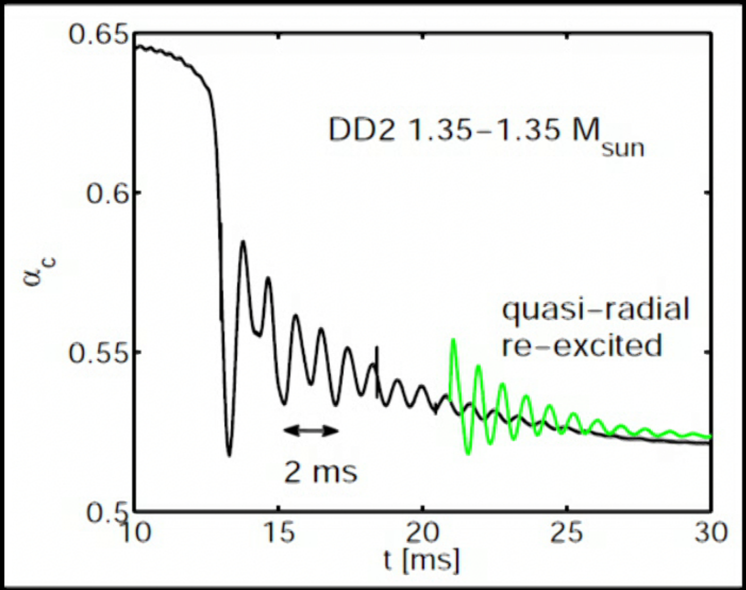

Bauswein et al. 2015

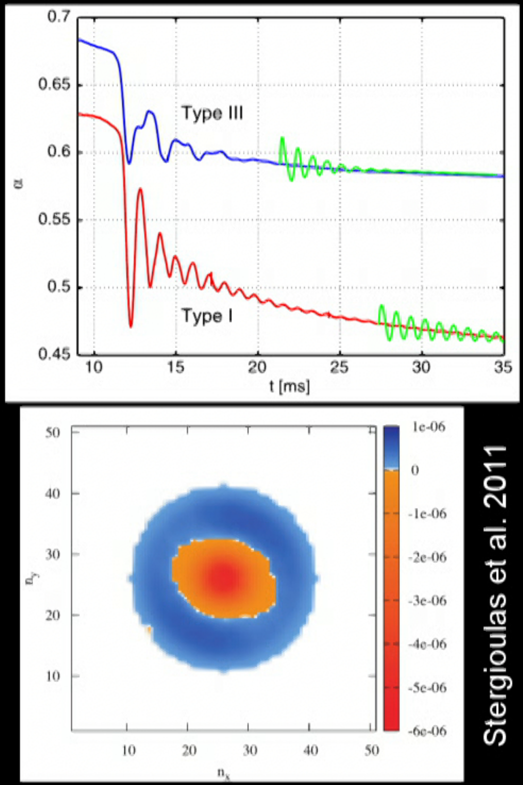

Stergioulas et al. 2011

Could consider also size of the remnant, rhomax, …

Note: additional low-frequency oscillation (500 Hz) also in GW amplitude (explained later)

Generic GW spectrum

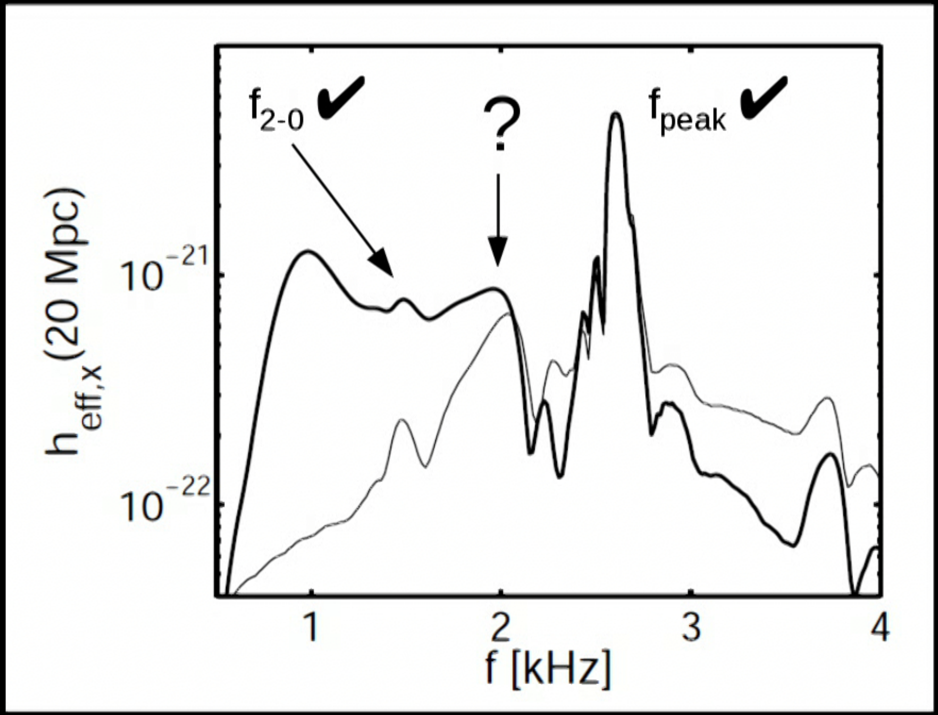

- Interaction between dominant quadrupolar mode and quasi-radial oscillation produced peak at $f_{2\text{-}0} = f_{peak} - f_0$ (see Stergioulas et al. 2011)

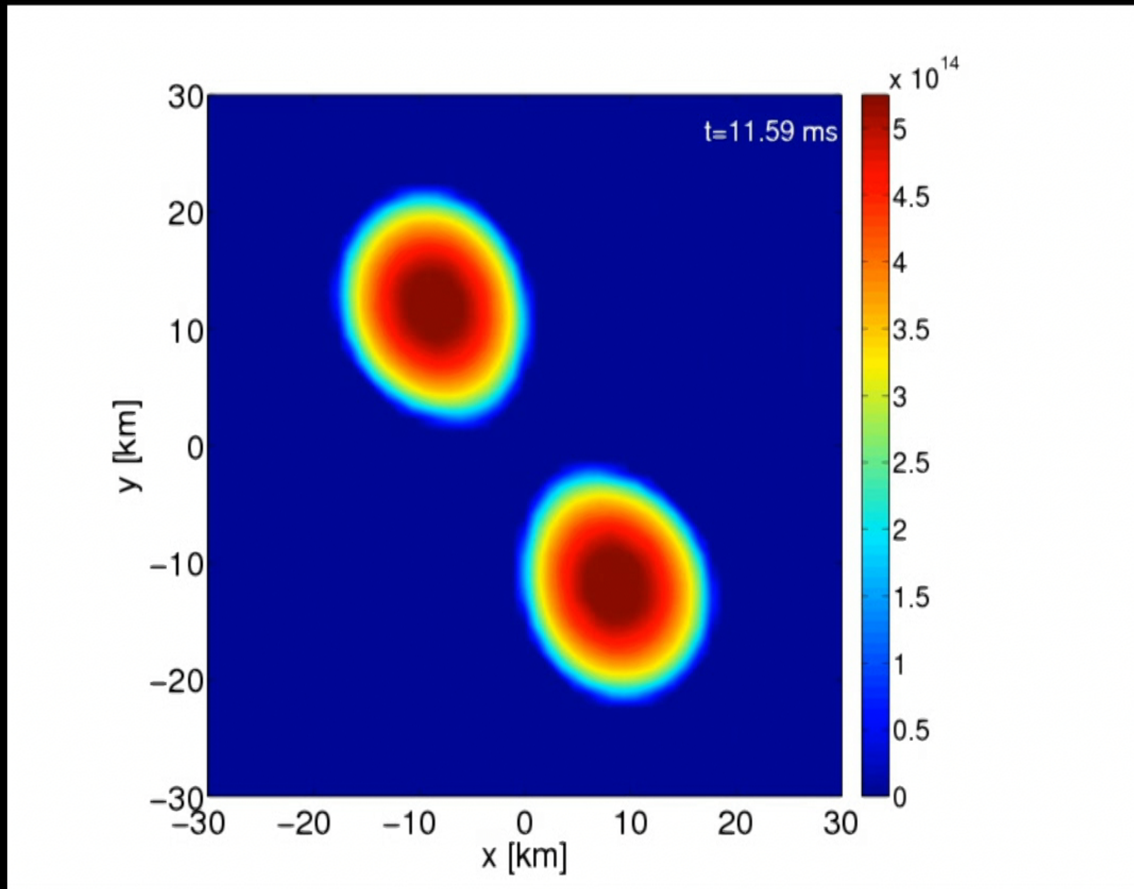
t=11.59 ms
x 10^14
5
4.5
4
3.5
3
2.5
2
1.5
1
0.5
0
30
20
10
0
−10
−20
−30
y [km]
−30
−20
−10
0
10
20
30
x [km]

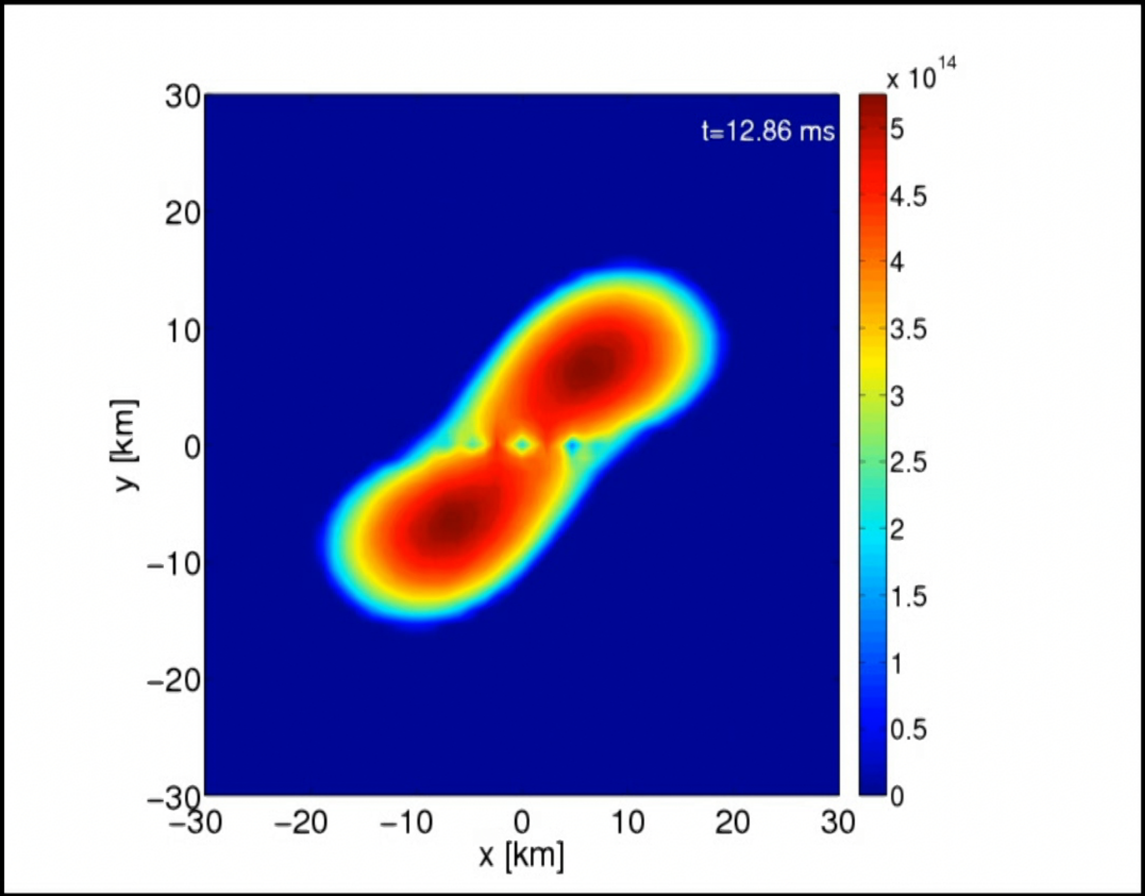
t=12.86 ms
x 10^14
5
4.5
4
3.5
3
2.5
2
1.5
1
0.5
0
30
20
10
0
−10
−20
−30
y [km]
−30
−20
−10
0
10
20
30
x [km]

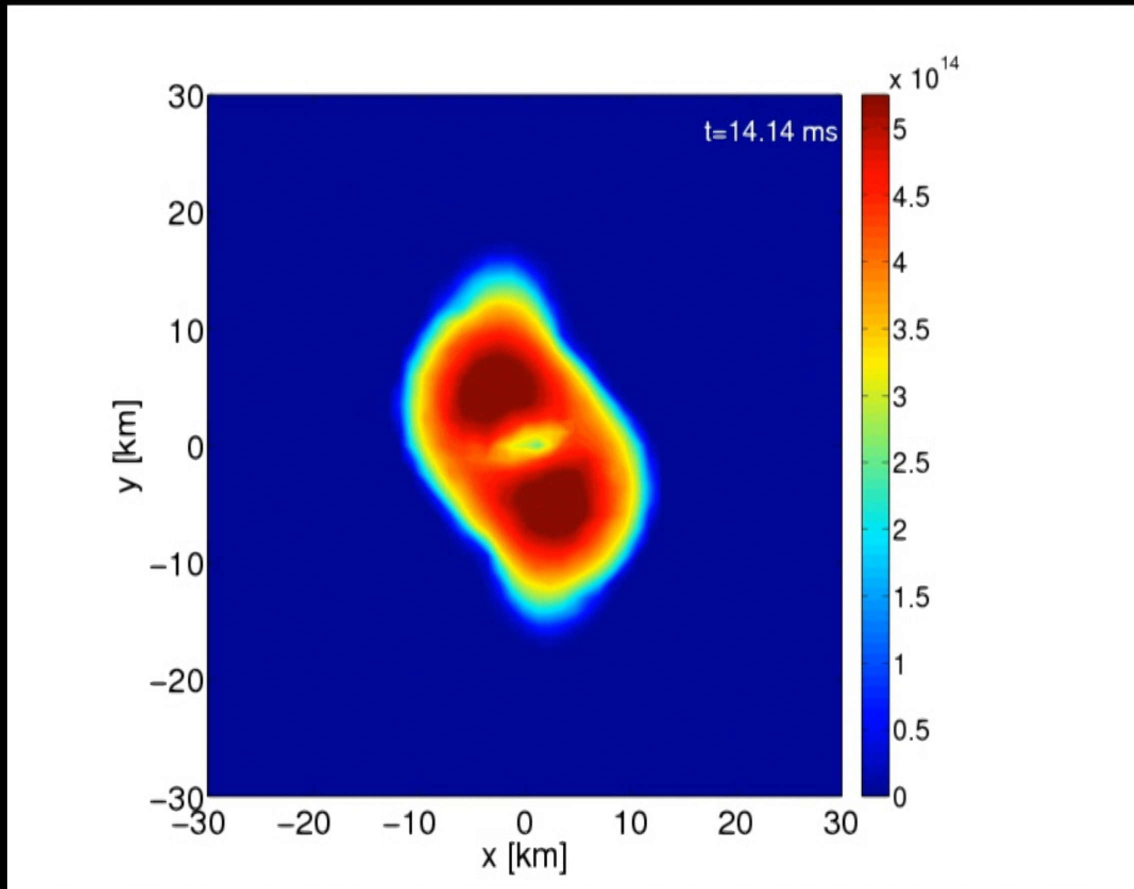

t=14.14 ms
x 10^14
y [km]
x [km]
30
20
10
0
−10
−20
−30
5
4.5
4
3.5
3
2.5
2
1.5
1
0.5

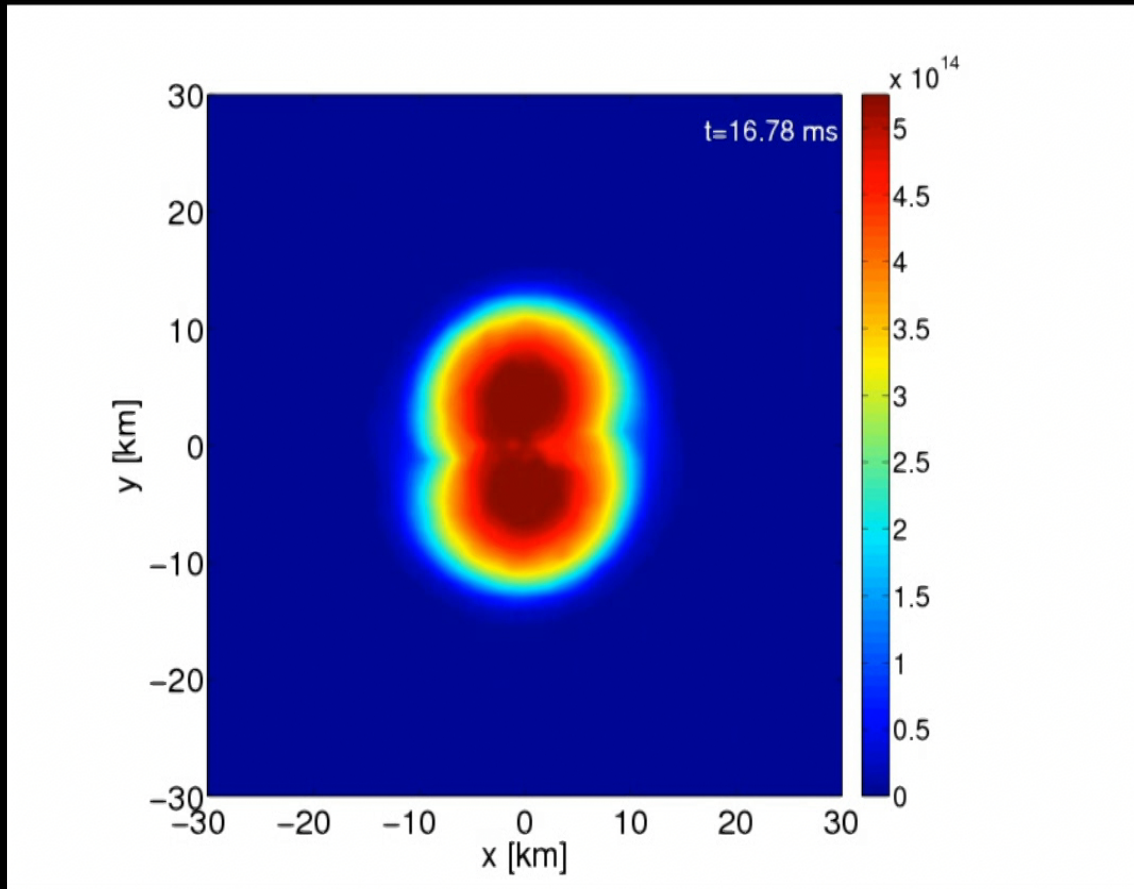

t=16.78 ms
x 10^14
5
4.5
4
3.5
3
2.5
2
1.5
1
0.5
0
30
20
10
0
−10
−20
−30
y [km]
−30
−20
−10
0
10
20
30
x [km]

Antipodal bulges (spiral pattern)

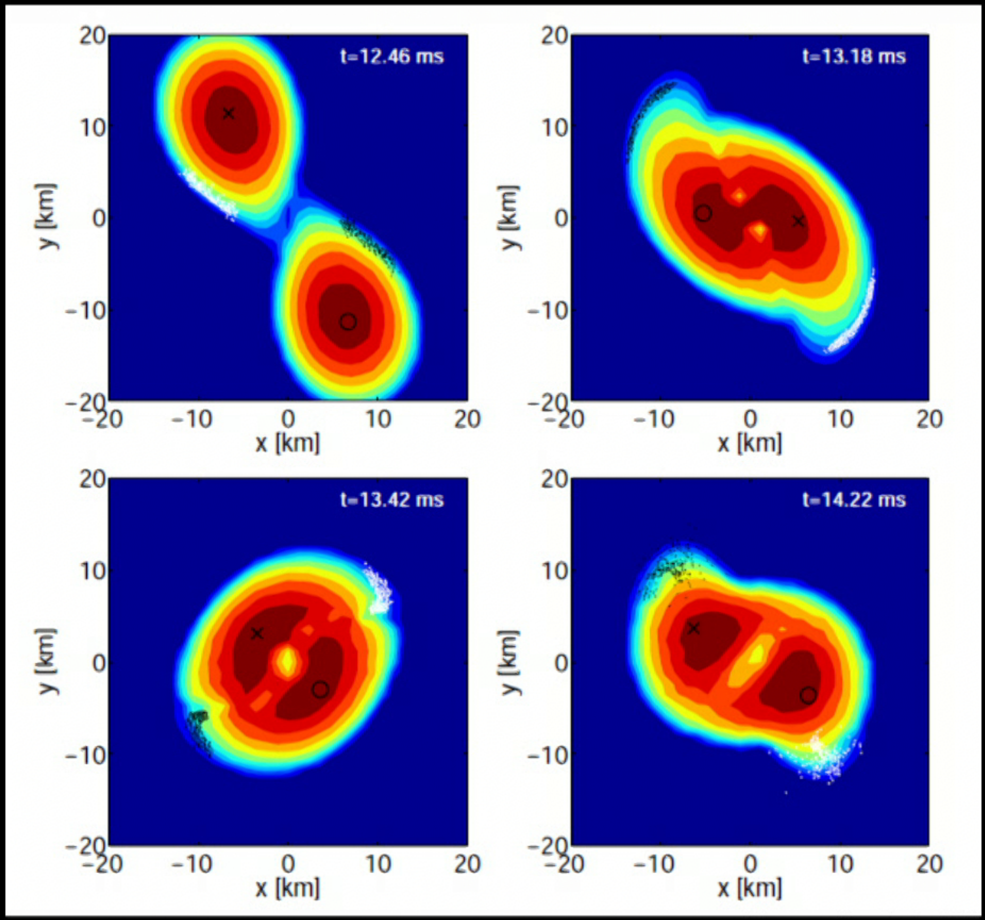

Bauswein et al. 2015

Orbital motion of antipodal bulges slower than inner part of the remnant (double-core structure)

Spiral pattern, created during merging lacks behind

Orbital frequency: 1/1ms → generates GW at 2 kHz !!!

Present for only a few ms / cycles

Generic GW spectrum

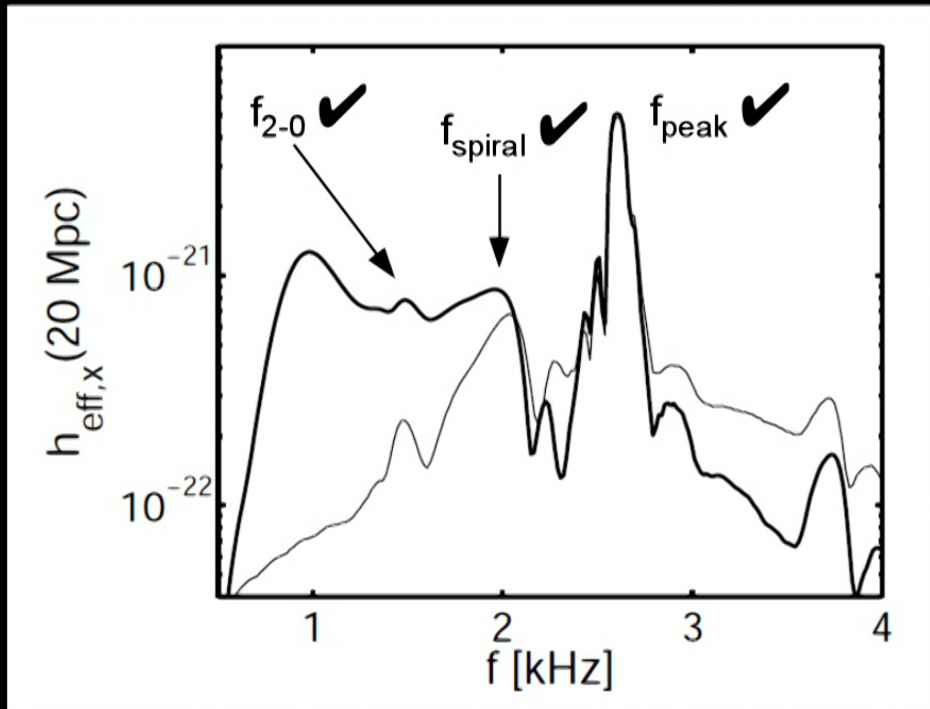

- Orbital motion of antipodal bulges generate peak at f_{spiral}

Further evidence

- Presence of spiral pattern coincides with presence of peak in GW spectrum (different time windows for FFT)
- Mass of bulges (several 0.1 M_{sun}) can explain strength of the peak by toy model of point particles the central remnant for a few ms
- Tracing dynamics / GW emission by computing spectra for “outer” and “inner” remnant → f_{spiral} emission “is produced outside”
- Dynamics of double cores (inner remnant) fail to explain this emission
- Spectrogram agrees with this picture (length, frequency), no strong time-variation of the dominant frequency

=> orbital motion => f_{spiral} peak

Example: TM1 1.35-1.35 Msun, strong tidal bulges, weak radial oscillation (e.g. from analysis of lapse)

Clark et al. 2016

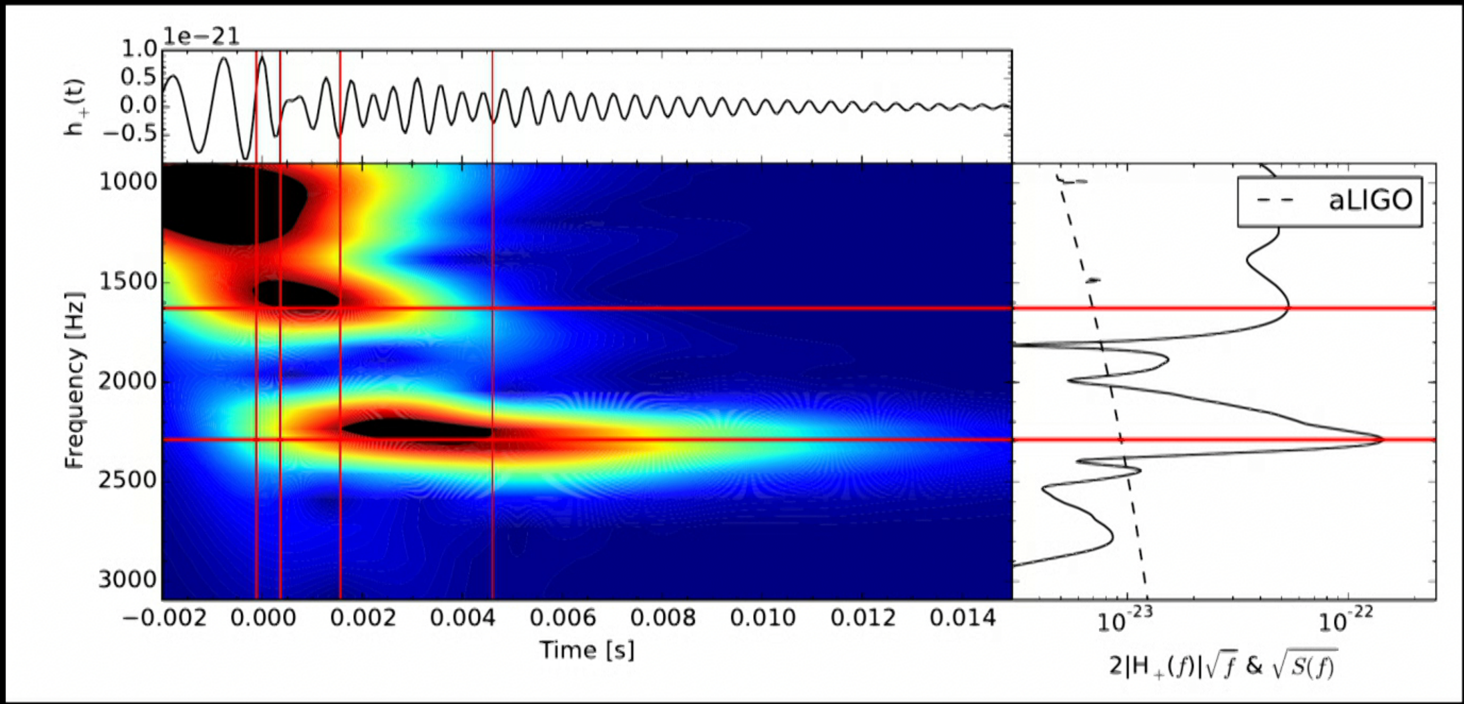

SFHO 1.35-1.35 Msun, weak tidal bulges, strong radial oscillation

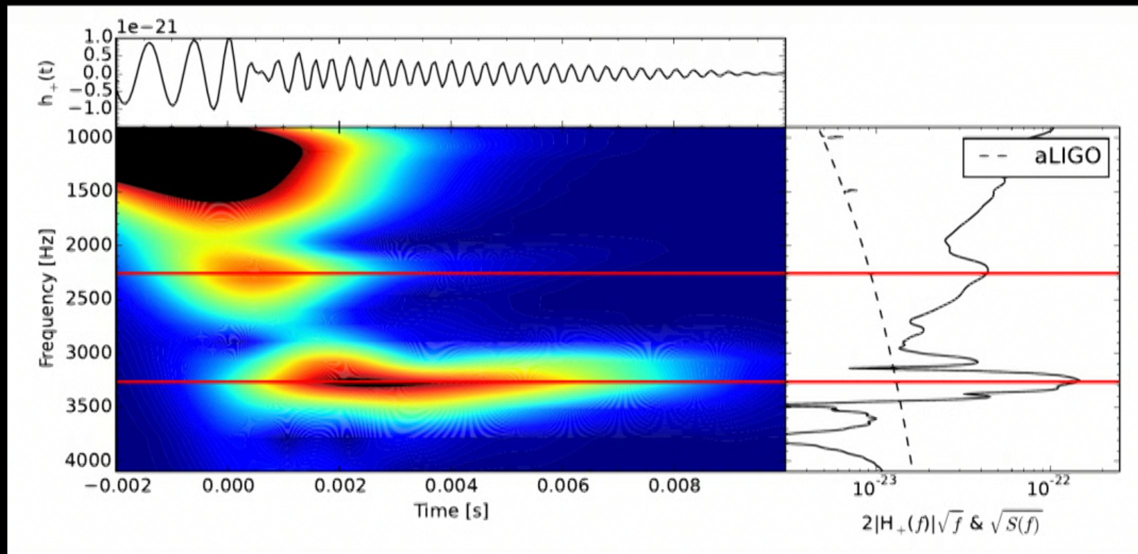

Clark et al. 2016

Discrete features !

Unified picture of postmerger GW emission and dynamics – a classification scheme

Survey of GW spectra

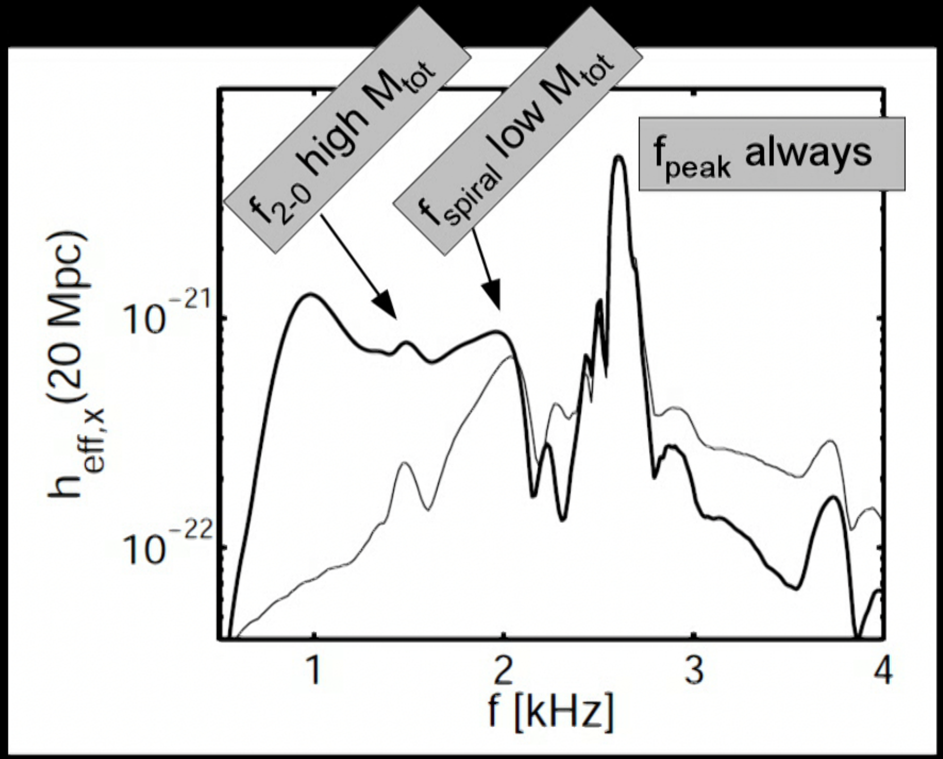

- Quantitative analysis of many models to identify which features is what
- Considering different models (EoS, M_{tot}): 3 types of spectra depending on presence of secondary features (dominant f_{peak} is always present)

Bauswein & Stergioulas 2015

Survey of GW spectra

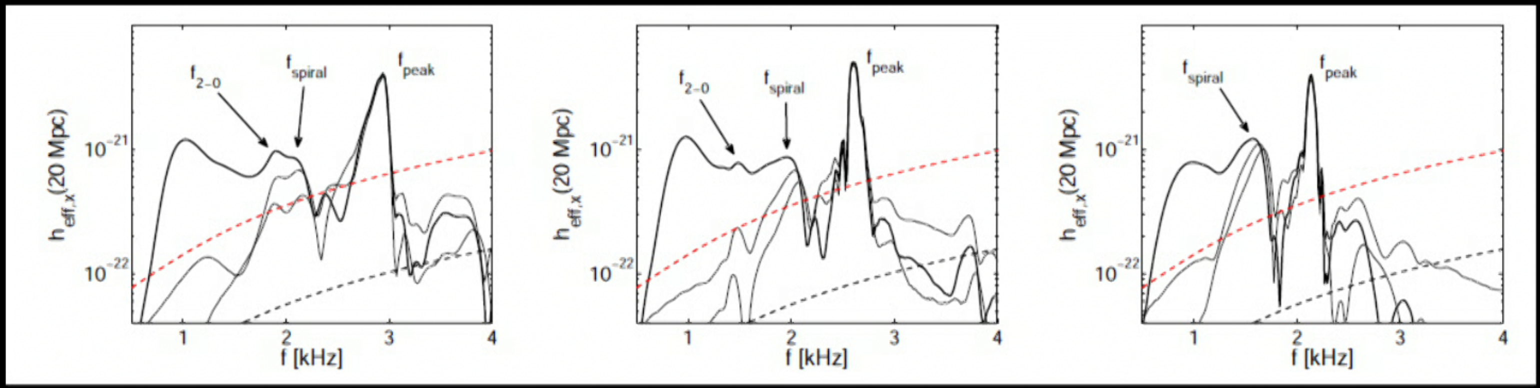

Type I Type II Type III

LS220, DD2, NL3 EoS all with M_{tot} = 2.7 M_{sun} → consider M_{tot} relative M_{thres}

=> Depending on binary model (EoS, M1/2) either one or the other or both features are present / dominant

Postmerger dynamics

- Different types also reflected in dynamics – clear from underlying mechanisms

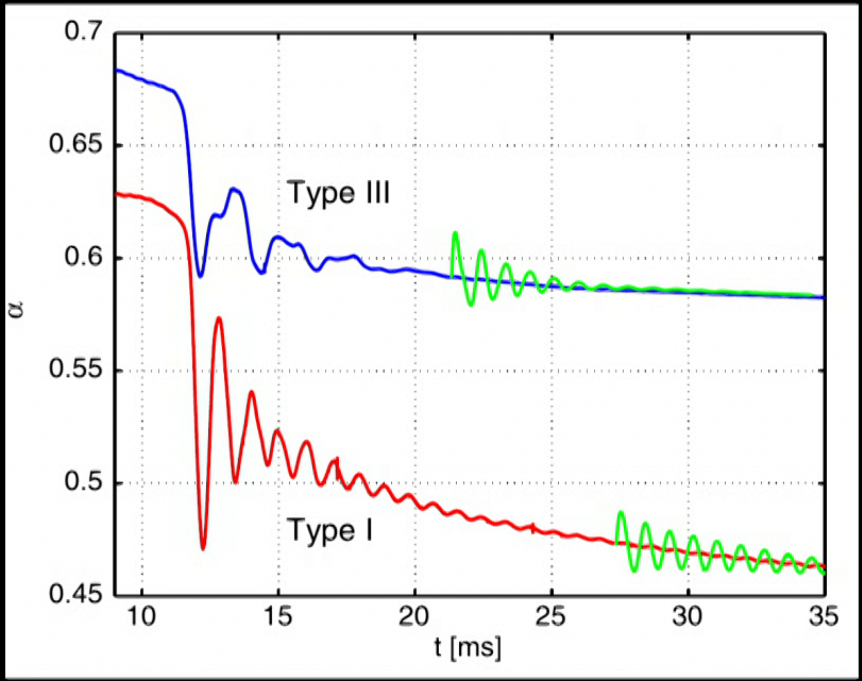

Classification scheme

- Type I: 2-0 feature dominates, f_{spiral} hardly visible, radial mode strongly excited, observed for soft EoS, relatively high M_{tot}
- Type II: both secondary features have comparable strength, clearly distinguishable, moderate binary masses
- Type III: f_{spiral} dominates, $f_{2\text{-}0}$ hardly visible, found for stiff EoS, relatively low binary masses, (central lapse, GW amplitude, rhomax show low-frequency modulation in addition to radial oscillation)

- Different types show also different dynamical behavior, e.g. in central lapse, maximum density, GW amplitude, ...
- High mass / low mass relative to threshold binary mass for prompt BH collapse (→ EoS dependent)
- Continuous transition between different types: a given EoS shows all types depending on M_{tot}: Type III for low M_{tot} → Type I towards M_{thres}

Bauswein & Stergioulas 2015

Classification scheme

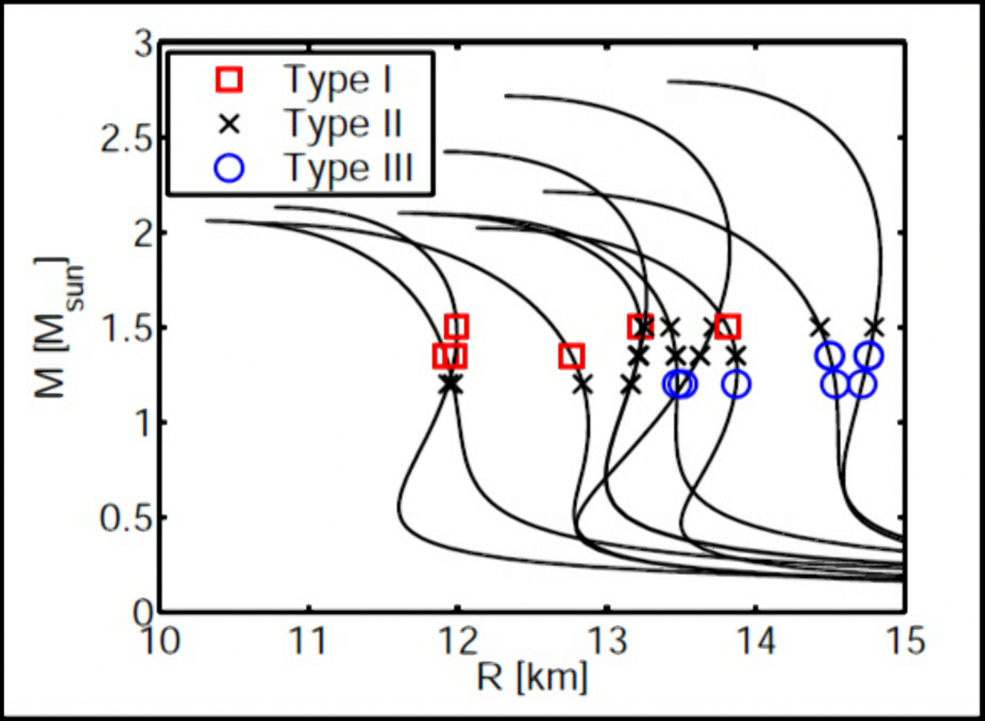

Type of M_1-M_2 merger indicate at $M_{tot}/2 = M_1$

Bauswein et al. 2015

(Continuous transition between types → tentative association)

For $M_{tot} = 2.7\ M_{sun}$ all Types are possible depending on EoS

Classification intuitive: merger dynamics affected by compactness

Classification scheme

- Behavior understandable:

- Type I: compact NSs merge → high impact velocity / violent collision => radial oscillation strongly excited (2-0 dominant); higher compactness → formation of tidal bulges suppressed (f_{spiral} weaker)

- Type III: less compact NSs merge → lower impact velocity / smooth merging => radial mode suppressed (no 2-0); pronounced tidal bulges (strong f_{spiral} feature)

- For Type III and Type II low-frequency modulation with $f_{low} = f_{peak} - f_{spiral}$ by orientation of bulge w. r. t. inner double-core/bar

- (seen in lapse, GW amp., rhomax, ...)

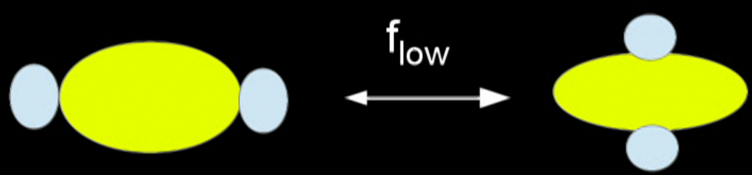

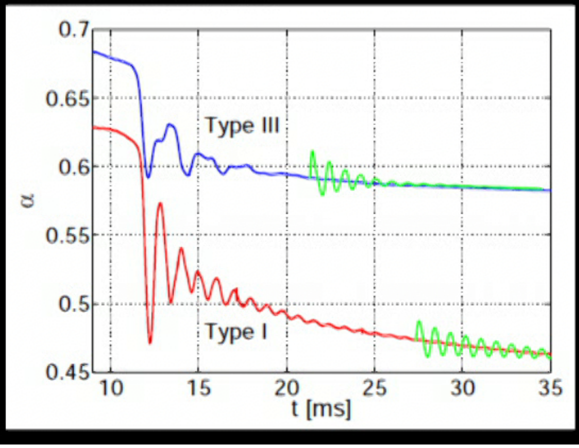

Dependencies of secondary features

Dependencies of secondary frequencies

EoS characterized by compactness C=M/R of inspiralling stars (equivalent to radius as before)

Bauswein et al. 2015

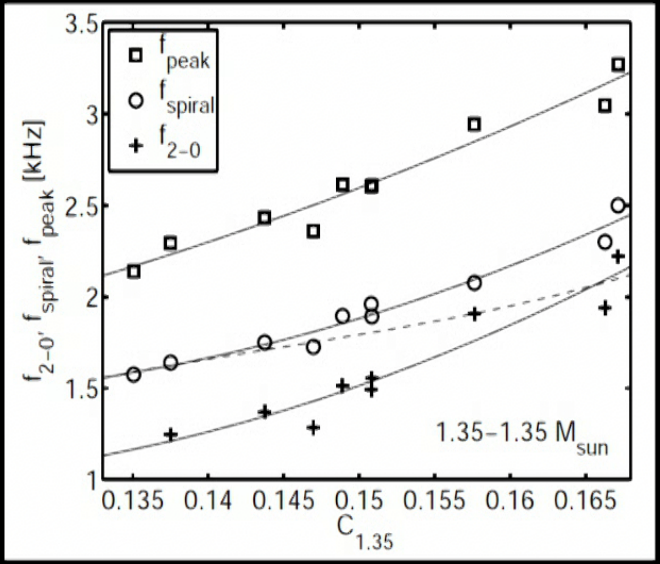

For fixed M_{tot} = 2.7 M_{sun}

Dashed line from Takami et al. 2014

- All three frequencies scale similarly with compactness (equivalently radius since M = $M_{tot}/2$ = fixed here)
- If subdominant peaks with comparable strength → risk of confusion / misinterpretation of measured frequency
- Here: only temperature-dependent EoS to avoid uncertainties/ambiguities due to approximate treatment of thermal effects (Gamma_th)
- For small binary mass asymmetry only small quantitative shifts
-

Different binary masses

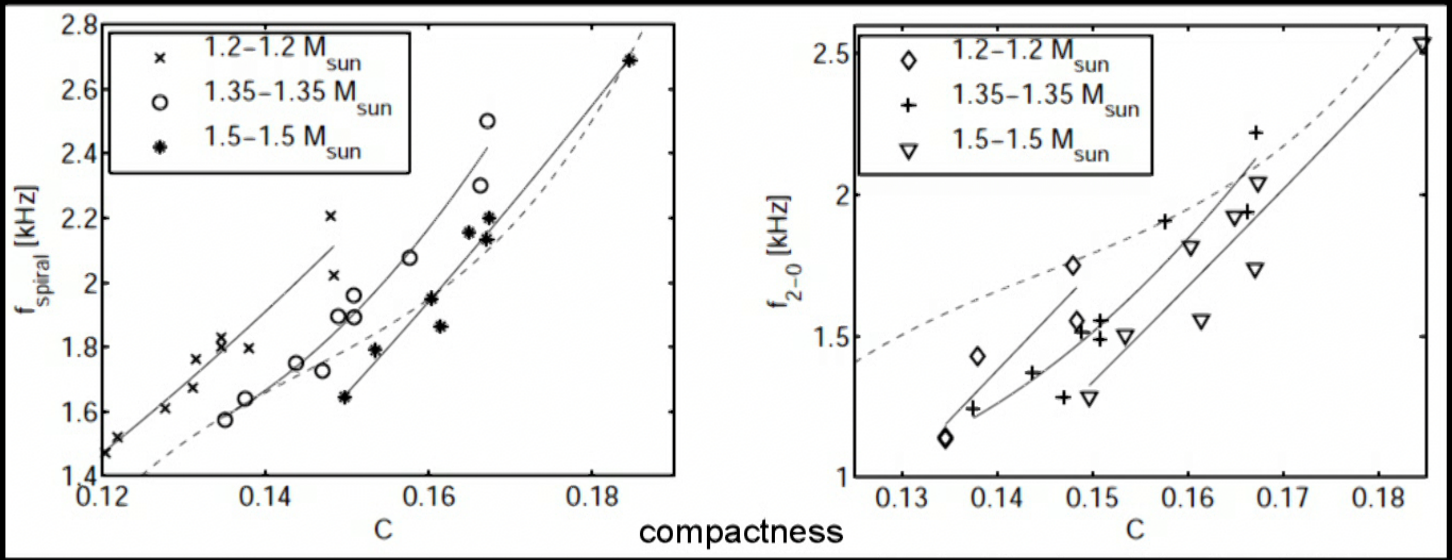

Bauswein et al. 2015

Dashed line from Takami et al. 2014

- for the individual secondary frequencies there are relations between C and the frequency for fixed binary masses (solid lines)
- (binary masses will be known from GW inspiral signal)
- no single, universal, mass-independent relation (for a expected range of binary masses), also when choosing the strongest secondary peak (risk of confusing subd. peaks)

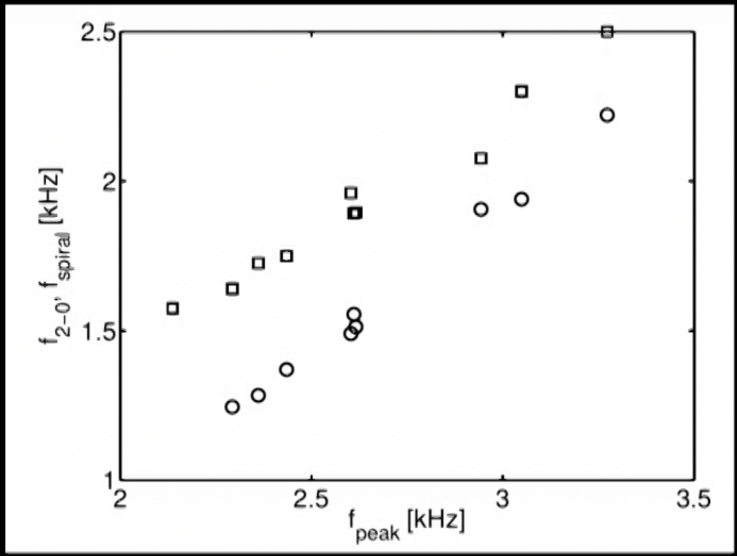

1.35-1.35 Msun

Clark et al. 2016

→ secondary frequencies are essentially given by dominant frequency

Collapse behavior

→ from latest detection: very robust lower limit on NS radius (complementary to upper bound from inspiral)

→ maximum mass of non-rotating NSs →very high density regime

→ also relevant for mass ejection, em counterpart, GRB

Collapse behavior: Prompt vs. delayed (/no) BH formation

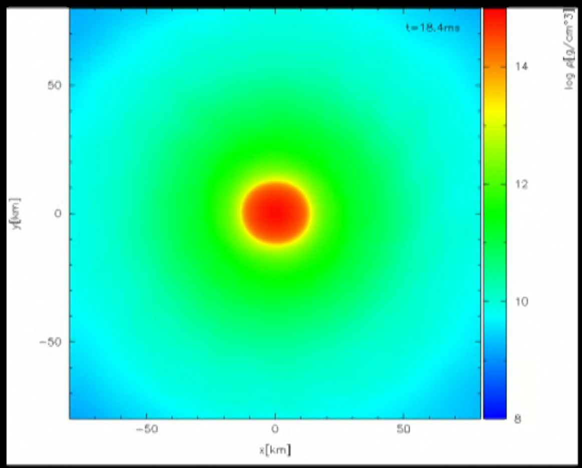

$M_{\rm tot} = 3.4\ M_\odot$ ←

$M_{\rm tot} = 3.5\ M_\odot$ →

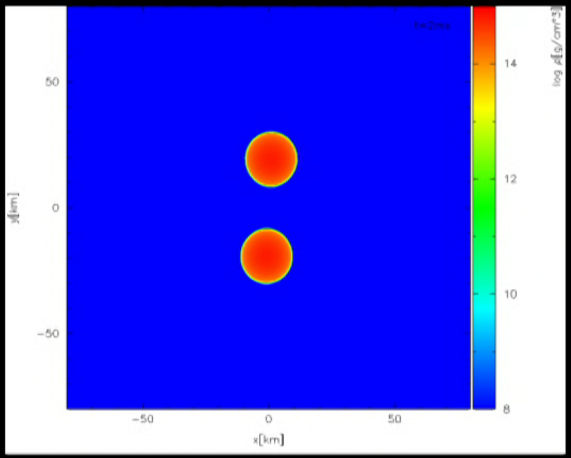

Shen EoS

$$\Rightarrow \quad M_{\rm thres} \approx 3.45\ M_\odot$$

Collapse behavior

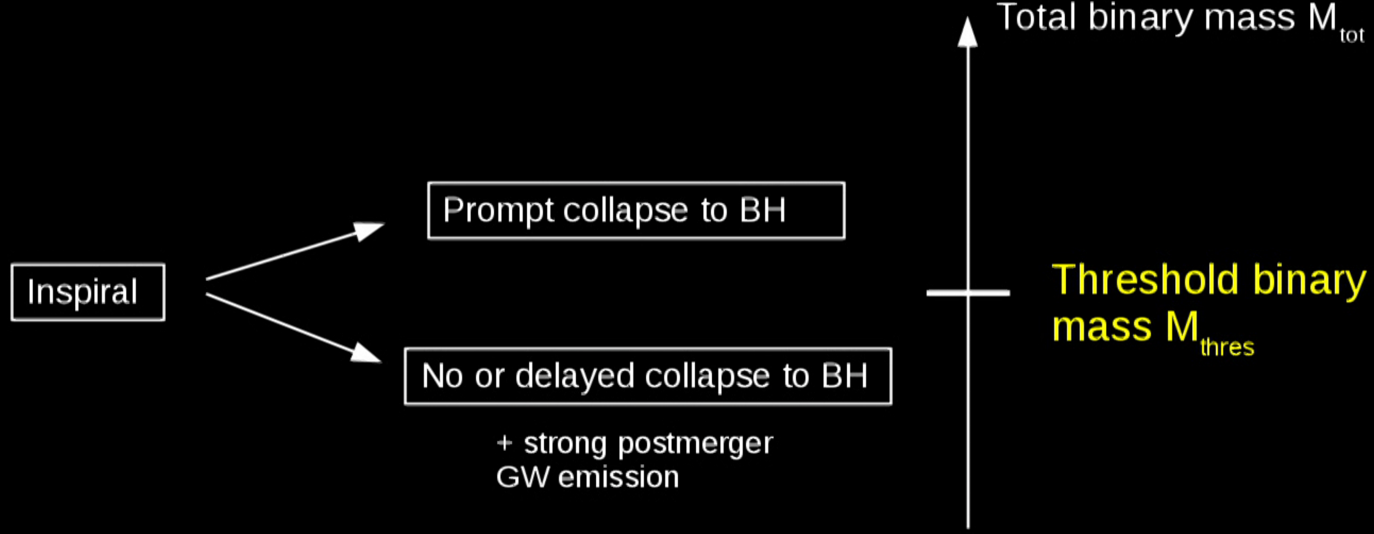

EoS dependent - somehow M_{max} should play a role

Simulations reveal M_{thres}

EoS	M_{max} ($M_\odot$)	R_{max} (km)	C_{max}	$R_{1.6}$ (km)	M_{thres} ($M_\odot$)
NL3 [37,38]	2.79	13.43	0.307	14.81	3.85
GS1 [39]	2.75	13.27	0.306	14.79	3.85
LS375 [40]	2.71	12.34	0.325	13.71	3.65
DD2 [38,41]	2.42	11.90	0.300	13.26	3.35
Shen [42]	2.22	13.12	0.250	14.46	3.45
TM1 [43,44]	2.21	12.57	0.260	14.36	3.45
SFHX [45]	2.13	10.76	0.292	11.98	3.05
GS2 [46]	2.09	11.78	0.262	13.31	3.25
SFHO [45]	2.06	10.32	0.294	11.76	2.95
LS220 [40]	2.04	10.62	0.284	12.43	3.05
TMA [44,47]	2.02	12.09	0.247	13.73	3.25
IUF [38,48]	1.95	11.31	0.255	12.57	3.05

Bauswein et al. 2013

Smooth particle hydrodynamics + conformal flatness

Threshold binary mass

- Empirical relation from simulations with different M_{tot} and EoS
- Fits (to good accuracy):

$$M_{\rm thres} = M_{\rm thres}(M_{\rm max}, R_{\rm max}) = \left(-3.38\frac{GM_{\rm max}}{c^2 R_{\rm max}} + 2.43\right) M_{\rm max}$$

$$M_{\rm thres} = M_{\rm thres}(M_{\rm max}, R_{1.6}) = \left(-3.6\frac{G\,M_{\rm max}}{c^2\,R_{1.6}} + 2.38\right) M_{\rm max}$$

- Both better than 0.06 M_{sun}

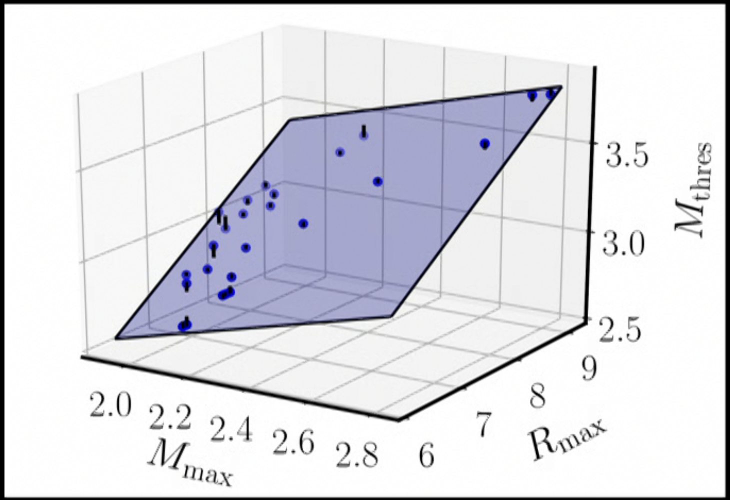

A simple but robust NS radius constraint from GW170817

- High ejecta mass inferred from electromagnetic transient

  → provides strong support for a delayed/no collapse in GW170817

  → even asymmetric mergers that directly collapse do not produce such massive ejecta

Reference	$m_{\rm dyn}\,[M_\odot]$	$m_{\rm w}\,[M_\odot]$
Abbott et al. (2017a)	0.001 – 0.01	–
Arcavi et al. (2017)	–	0.02 – 0.025
Cowperthwaite et al. (2017)	0.04	0.01
Chornock et al. (2017)	0.035	0.02
Evans et al. (2017)	0.002 – 0.03	0.03 – 0.1
Kasen et al. (2017)	0.04	0.025
Kasliwal et al. (2017b)	> 0.02	> 0.03
Nicholl et al. (2017)	0.03	–
Perego et al. (2017)	0.005 – 0.01	10^{-5} – 0.024
Rosswog et al. (2017)	0.01	0.03
Smartt et al. (2017)	0.03 – 0.05	0.018
Tanaka et al. (2017a)	0.01	0.03
Tanvir et al. (2017)	0.002 – 0.01	0.015
Troja et al. (2017)	0.001 – 0.01	0.015 – 0.03

Compilation in Cote et al 2018

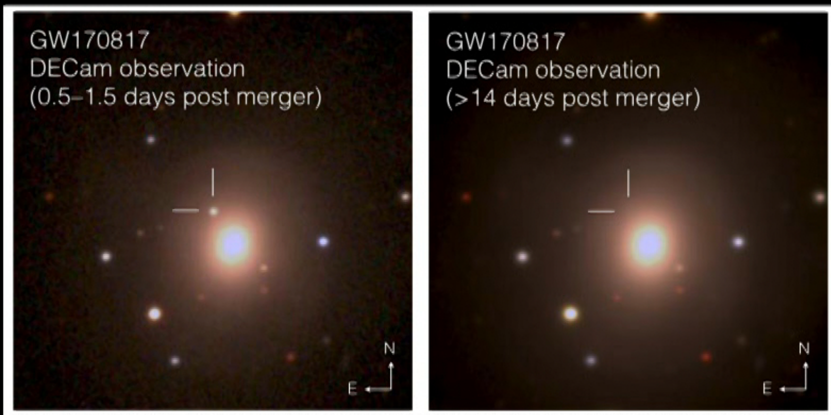

Figure 1. NGC4993 *grz* color composites (1!5 × 1!5). Left: composite of detection images, including the discovery *z* image taken on 2017 August 18 00:05:23 UT and the g and r images taken 1 day later; the optical counterpart of GW170817 is at R.A., decl. =197.450374, −23.381495. Right: the same area two weeks later.

Soares-Santos et al 2017

- Ejecta masses depend on EoS and binary masses
- Note: high mass points already to soft EoS (tentatively/qualitatively)
- Prompt collapse leads to reduced ejecta mass
- Light curve depends on ejecta mass:

  → 0.02 - 0.05 M_{sun} point to delayed collapse
- Note: here only dynamical ejecta

Only dynamical ejecta

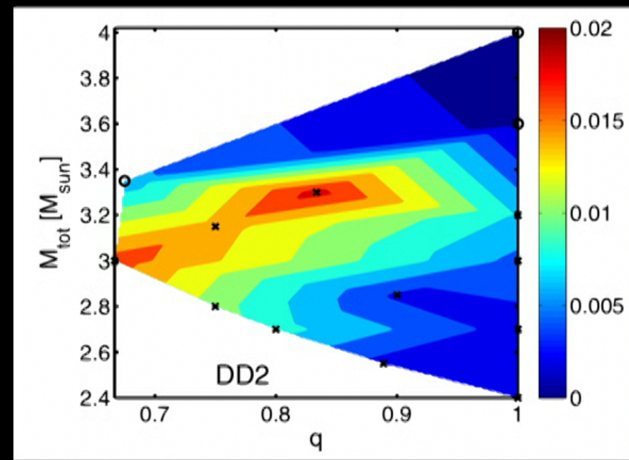

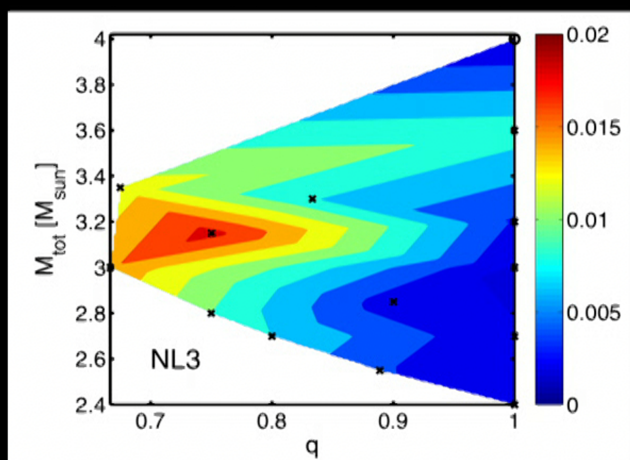

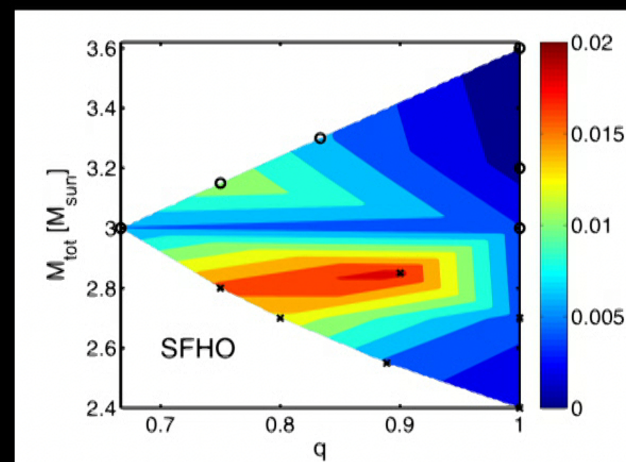

Bauswein et al. 2013

(1) If GW170817 was a delayed (/no) collapse:

$$M_{\rm thres} > M_{\rm tot}^{GW170817}$$

(2) Recall: empirical relation for threshold binary mass for prompt collapse:

$$M_{\rm thres} = \left(-3.38 \frac{G\, M_{\rm max}}{c^2\, R_{\rm max}} + 2.43\right) M_{\rm max} > 2.74\ M_\odot$$

(with M_{max}, R_{max} unknown)

(3) Causality: speed of sound $v_S \leq c$ $\Rightarrow M_{\rm max} \leq \frac{1}{2.82} \frac{c^2\, R_{\rm max}}{G}$

- Putting things together:

$$M_{\rm tot}^{GW170817} \leq \left(-3.38 \frac{G\, M_{\rm max}}{c^2\, R_{\rm max}} + 2.43\right) M_{\rm max} \leq \left(-\frac{3.38}{2.82} + 2.43\right) \frac{1}{2.82} \frac{c^2\, R_{\rm max}}{G}$$

→ Lower limit on NS radius

Bauswein et al. 2017

NS radius constraint from GW170817

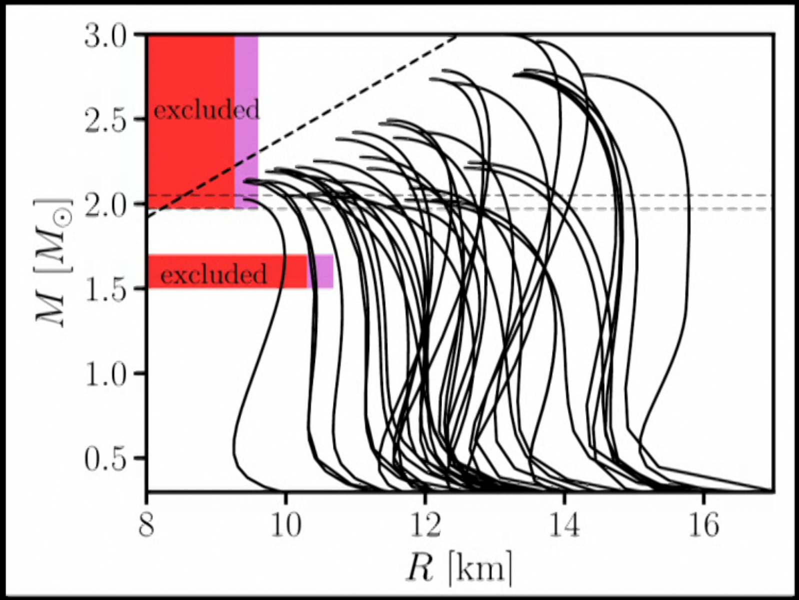

Bauswein et al. 2017

- $R_{1.6} > 10.7$ km
- Excludes very soft nuclear matter

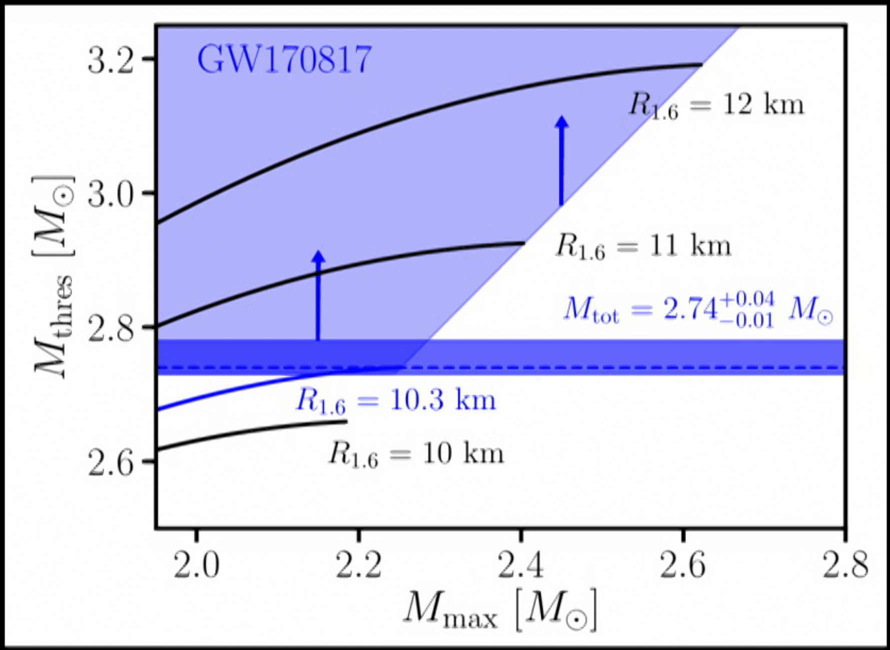

$$M_{\rm thres} = \left(-3.6\frac{G\,M_{\rm max}}{c^2\,R_{1.6}} + 2.38\right)\,M_{\rm max}$$

$$v_S = \sqrt{\frac{dP}{de}} \leq c \;\rightarrow\; M_{\rm max} \leq \kappa R_{1.6} \;\Rightarrow\; M_{\rm thres} \geq 1.2 M_{\rm max}$$

Discussion - robustness

- Binary masses well measured with high confidence error bar
- Clearly defined working hypothesis: delayed collapse

  → testable by refined emission models

  → as more events are observed more robust distinction

  → in future events presence of postmerger, i.e. kHz, GW emission will reveal nature of remnant
- Very conservative estimate, errors can be quantified
- Empirical relation can be tested by more elaborated simulations (but unlikely that MHD or neutrinos can have strong impact on M_{thres})
- Confirmed by semi-analytic collapse model
- Low-SNR constraint !!!

Future

- Any new detection can be employed if it allows distinction between prompt/delayed collapse
- With more events in the future our comprehension of em counterparts will grow → more robust discrimination of prompt/delayed collapse events
- Low-SNR detections sufficient !!! → that's the potential for the future

  → we don't need louder events, but more

  → complimentary to existing ideas for EoS constraints

Future detections (hypothetical discussion)

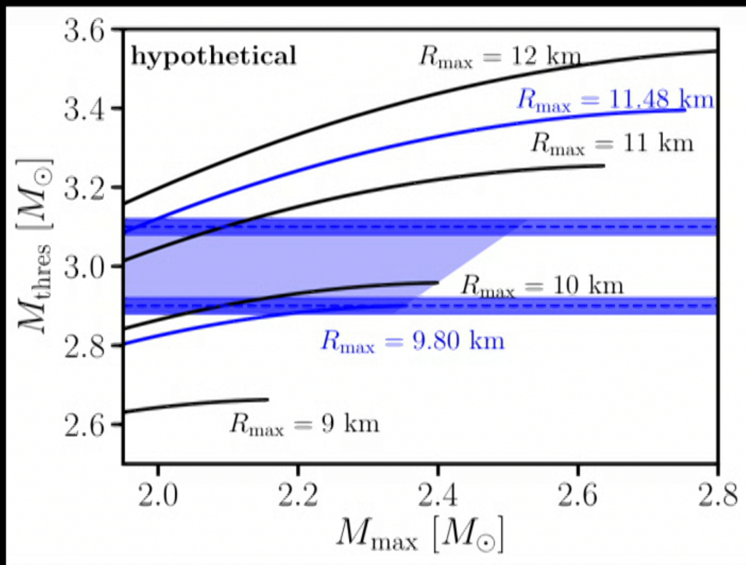

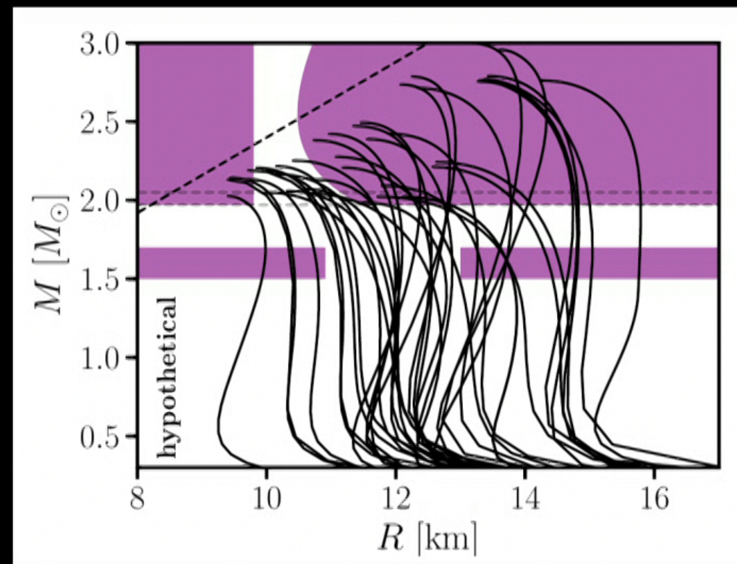

→ as more events are observed, bands converge to true M_{thres}

→ prompt collapse constrains M_{max} from above

Bauswein et al. 2017

Future: Maximum mass

- Empirical relation

$$M_{\rm thres} = \left(-3.6\frac{G\,M_{\rm max}}{c^2\,R_{1.6}} + 2.38\right)\,M_{\rm max}$$

- Sooner or later we'll know $R_{1.6}$ (e.g. from postmerger) and M_{thres} (from several events – through presence/absence of postmerger GW emission or em counterpart)

=> direct inversion to get precise estimate of M_{max}

(see also current estimates e.g. by Margalit & Metzger, Rezzolla et al, Ruiz & Shapiro, ...)

Alternative: f_{peak} dependence on total binary mass

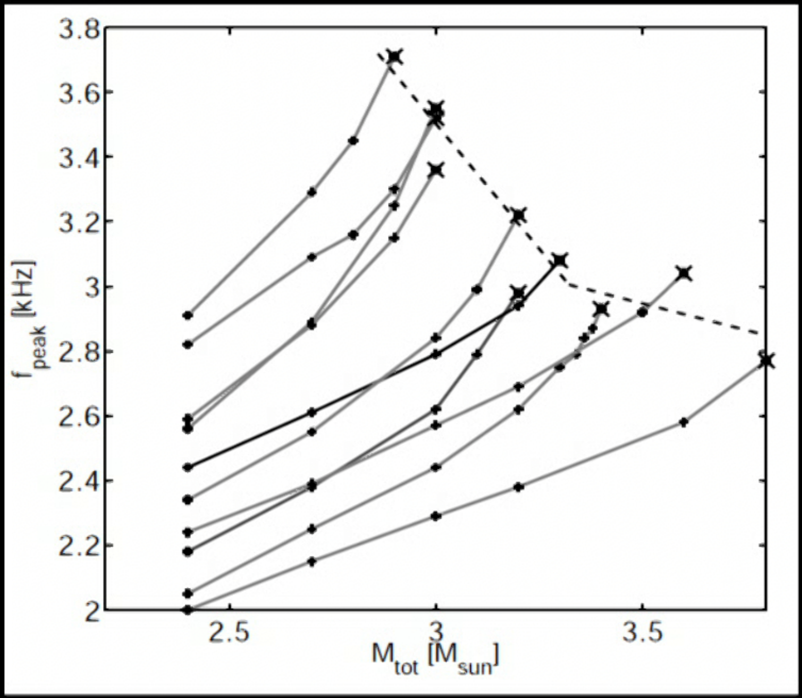

(every single line corresponds to a specific EoS → only one line can be the true EoS)

$$f_{peak} \sim \sqrt{\frac{M}{R^3}}$$

Bauswein et al. 2014

- Dominant GW frequency monotone function of M_{tot}
- Threshold to prompt BH collapse shows a clear dependence on M_{tot} (dashed line)

Maximum density from f_{thres}

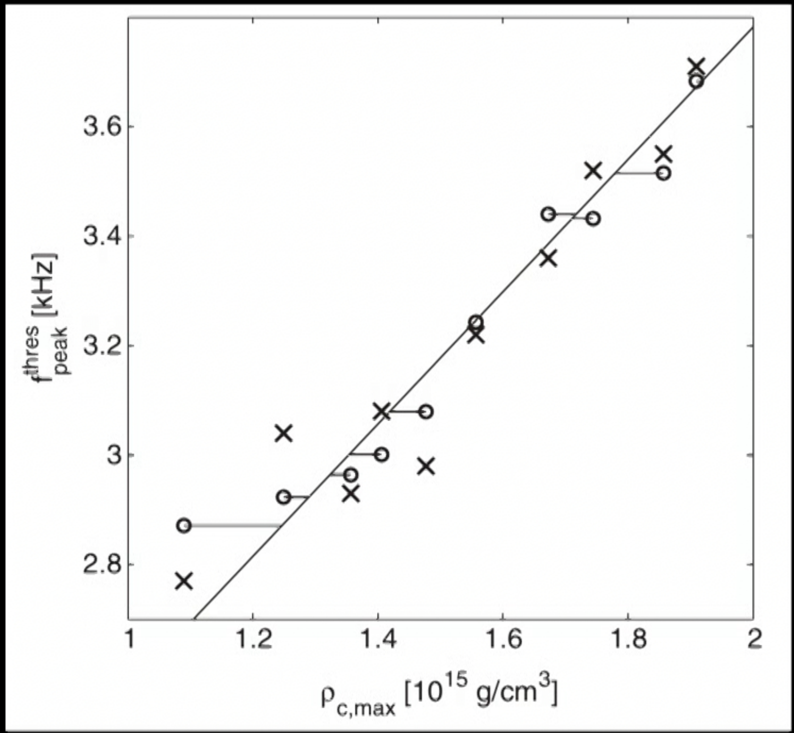

either through extrapolation or through direct measurement of f_{peak} close to threshold

Bauswein et al. 2014

from two measurements of f_{peak} at moderate M_{tot}

Maximum-mass TOV properties

by extrapolation of f_{peak} (M_{tot})

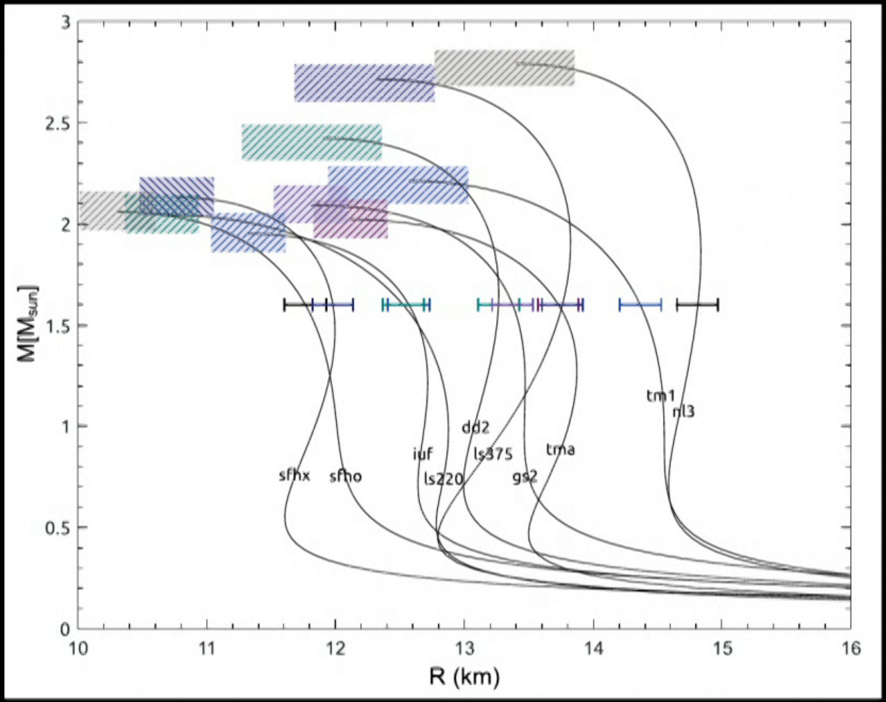

Radius at lower masses from f_{peak}

(final error will depend on EoS and exact systems measured)

Note: M_{thres} may also be constrained from prompt collapse directly

Bauswein et al. 2014

Conclusions / future potential

- Postmerger complementary to inspiral
- Dominant postmerger frequency → accurate radius measurement
- Through extrapolation procedure access to very high-density regime → M_{max}, R_{max}, e_{max}
- GW data analysis simulations → postmerger measurable
- Unified picture of postmerger GW emission, i.e. secondary features → encoding postmerger dynamics
- Collapse behavior of GW170817

  → robust lower bound on NS radius → $R > 10.7$ km

  → a lot of future potential → M_{max}

- Outlook: kHz range indispensable for multi-messenger picture of NS mergers

  understand all details of the GW spectrum → GW asteroseismology